Heme/Copper Terminal Oxidases

Shelagh Ferguson-Miller*

Department of Biochemistry, Michigan State University, East Lansing, Michigan 48824

Gerald T. Babcock*

Department of Chemistry, Michigan State University, East Lansing, Michigan 48824

Received August 6, 1996 (Revised Manuscript Received September 2, 1996)

Contents

A. Introduction

Spatially well-organized electron-transfer reactions in a series of membrane-bound redox proteins form the basis for energy conservation in both photosynthesis and respiration. The membrane-bound nature of the electron-transfer processes is critical, as the free energy made available in exergonic redox chemistry is used to generate transmembrane proton concentration and electrostatic potential gradients. These gradients are subsequently used to drive ATP formation, which provides the immediate energy source for constructive cellular processes.

The terminal heme/copper oxidases in respiratory electron-transfer chains illustrate a number of the thermodynamic and structural principles that have driven the development of respiration (see refs 1−6, for recent reviews). This class of enzyme reduces dioxygen to water, thus clearing the respiratory system of low-energy electrons so that sustained electron transfer and free-energy transduction can occur. By using dioxygen as the oxidizing substrate, free-energy production per electron through the chain is substantial, owing to the high reduction potential of O_2 (0.815 V at pH 7). For example, if the initial electron donor is NADH, more than 1.1 eV/electron through the respiratory chain is available for ATP synthesis. Moreover, the dioxygen binding and activating site in the terminal oxidases, which comprises the binuclear heme a_3/Cu_B center (section B), is ideally suited to using O_2 as an oxidizing substrate. Very little leakage of potentially damaging, partially reduced oxygen species ($O_2^{\bullet -}$, O_2^{2-}, $OH^{\bullet}$) occurs from this site; recent work implicates the quinone cofactors as the principal loci for the generation of reactive oxygen species in the respiratory process.[7]

The high-spin heme/Cu_B site is also constructed so as to operate dioxygen reduction at low overpotential. As opposed to most electrochemical methods for dioxygen reduction, where overpotentials greater than 1 V are commonly encountered, the dioxygen overpotential in the terminal oxidases is less than 0.3 V. This feature of the binuclear center is critical in maximizing respiratory free-energy production. Firstly, it allows the use of fairly high potential reductants as its electron source: in the cytochrome *c* oxidases, the potential of the cytochrome *c* donor is 250 mV; in the quinol terminal oxidases, the quinol potential is only ∼200 mV more negative. The net result of these energetics is that the driving force available for redox-linked proton translocation in regions of the respiratory chain prior to the terminal oxidase is maximized. Secondly, the low overpotential associated with O_2 reduction, in concert with the vectorial nature of electron transfer through the enzyme, allows the terminal oxidases themselves to contribute directly to the transmembrane free-energy gradient, that is, they operate as redox-linked proton pumps.[8] The proton-translocating activity of the enzyme occurs with a stoichiometry that approaches one proton pumped per electron delivered to dioxygen. Thus, we can write the overall reaction catalyzed by the terminal oxidases as

$$4D_{red} + O_2 + 8H^+_{in} \rightarrow 4D_{ox} + 2H_2O + 4H^+_{out}$$

where D_{red} and D_{ox} represent the reduced and oxidized forms of the immediate electron donors to the

S0009-2665(95)00051-3 CCC: $25.00

Shelagh Ferguson-Miller is Professor and Associate Chair of Biochemistry at Michigan State University. Born in Toronto, Canada, she did undergraduate studies at the University of Toronto in Physiology and Biochemistry. She received a Master's degree in Biochemistry from the University of Toronto in 1966 and a Ph.D. in Biochemistry in 1971 with Henry Lardy at the Enzyme Institute, University of Wisconsin, Madison. After postdoctoral studies with George Radda at Oxford University, U.K., and Emmanuel Margoliash at Northwestern University, Evanston, IL, she was appointed Assistant Professor of Biochemistry at Michigan State University in 1978. Current research interest is in the area of bioenergetics: electron and proton translocation in cytochrome *c* oxidase, cytochrome *c* docking with cytochrome oxidase, and design and analysis of detergents for crystallizing membrane proteins. Publications include over 75 papers in refereed journals. She is on the editorial boards of *Biochimica et Biophysica Acta* and the *Journal of Bioenergetics and Biomembranes* and is Chairperson of the Gordon Conference on Bioenergetics in 1997. She has recently received the Distinguished Faculty Award from Michigan State University.

Gerald T. Babcock was born in Minneapolis, MN. He did his undergraduate work at Creighton University in Omaha, NB, where an interest in chemistry developed that was sparked in high school. Professors Zebolsky, Snipp, and Takamura were instrumental in focusing this interest toward the exploration of biological phenomena with physical chemical approaches. At the University of California, Berkeley, he did his graduate work under the guidance of Professor Ken Sauer and became fascinated with photosynthetic processes, particularly the photochemical and chemical reactions that produce O_2 from water. He stayed in Berkeley for an additional year after receiving his Ph.D. in 1973 and then moved, as an NIH postdoctoral fellow, to Professor Graham Palmer's lab at Rice University, where he studied the other half of the water/oxygen cycle in Nature, i.e., the reduction of O_2 to water by cytochrome oxidase. In 1976, he moved to Michigan State University, where he is now Professor and Chairman in the Department of Chemistry. He continues his interests in the biological aspects of water/oxygen chemistry and uses spectroscopic techniques, primarily Raman and electron magnetic resonance, to obtain deeper insights into the metabolism of this redox couple in a variety of enzymes. At present, he is an Associate Editor of the *Annual Reviews of Physical Chemistry* and a member of the Editorial Advisory Board for *Biochemistry*. He was a visiting professor at the College de France and a Phillips Lecturer at Haverford College. His interests outside science include bicycling, squash, and white-water canoeing, the latter of which he shares on a regular basis with members of his research group.

enzyme and H^+_{in} and H^+_{out} indicate that protons are taken up and released vectorially with respect to the respiratory membrane.

The past 4 years have seen rapid developments in our understanding of the inner working of this remarkable class of enzyme. The enzyme from two sources has been crystallized and its structure determined to high resolution. In fact, the local structure about the metal centers in subunit I determined by mutagenesis/spectroscopic approaches predated that of the crystal structures and correctly predicted the amino acid ligands to the redox cofactors in the resting form of the enzyme. Concomitant with the structural and mutagenetic progress has been the rapid development of time-resolved spectroscopic techniques that have provided deep insight into mechanistic aspects of the functional events catalyzed by the enzyme. Although progress in understanding the operation of the enzyme has been substantial, there are a number of areas, particularly those relating to the interplay between proton and electron currents, in which our ability to link observed phenomena to structure and activity of the protein is only rudimentary. In this review, we will summarize the progress that has been made, identify areas in which consensus is emerging, and, finally, indicate those aspects of enzyme function that remain problematic.

B. Insights from the Atomic Resolution Structures of Cytochrome c Oxidases

The commonality of the electron-transfer systems in eukaryotes and prokaryotes was observed by Keilin in 1925,[9] but only in the past 10 years have investigators exploited this fact, using the structurally simpler, genetically accessible bacterial systems to study the mechanism of energy transduction. In the case of cytochrome oxidase, this approach has led to major advances in our understanding of structure and mechanism, through the use of mutagenesis combined with spectroscopy and ultimately crystallography, culminating in the recent, successful solution of a 2.8 Å resolution X-ray structure of a bacterial cytochrome *c* oxidase.[10] This amazing feat was matched by the simultaneous achievement of an atomic-level resolution structure of the 13 subunit mammalian cytochrome *c* oxidase.[11,12] Coincident with these landmarks in membrane protein crystallography was the determination of a 2.5 Å structure of a soluble domain of oxidase containing an engineered Cu_A center.[13]

This sudden wealth of structural information has had, and will have, an enormous impact on the field. Although analysis of site-directed mutants successfully predicted many aspects of the active site structure, of the positions of metal centers in the protein,[14,15] and of the key residues in likely proton channels,[16−18] confirmation and extension of these pieces of knowledge by a complete structure provides the basis for far more powerful analysis of mechanism.

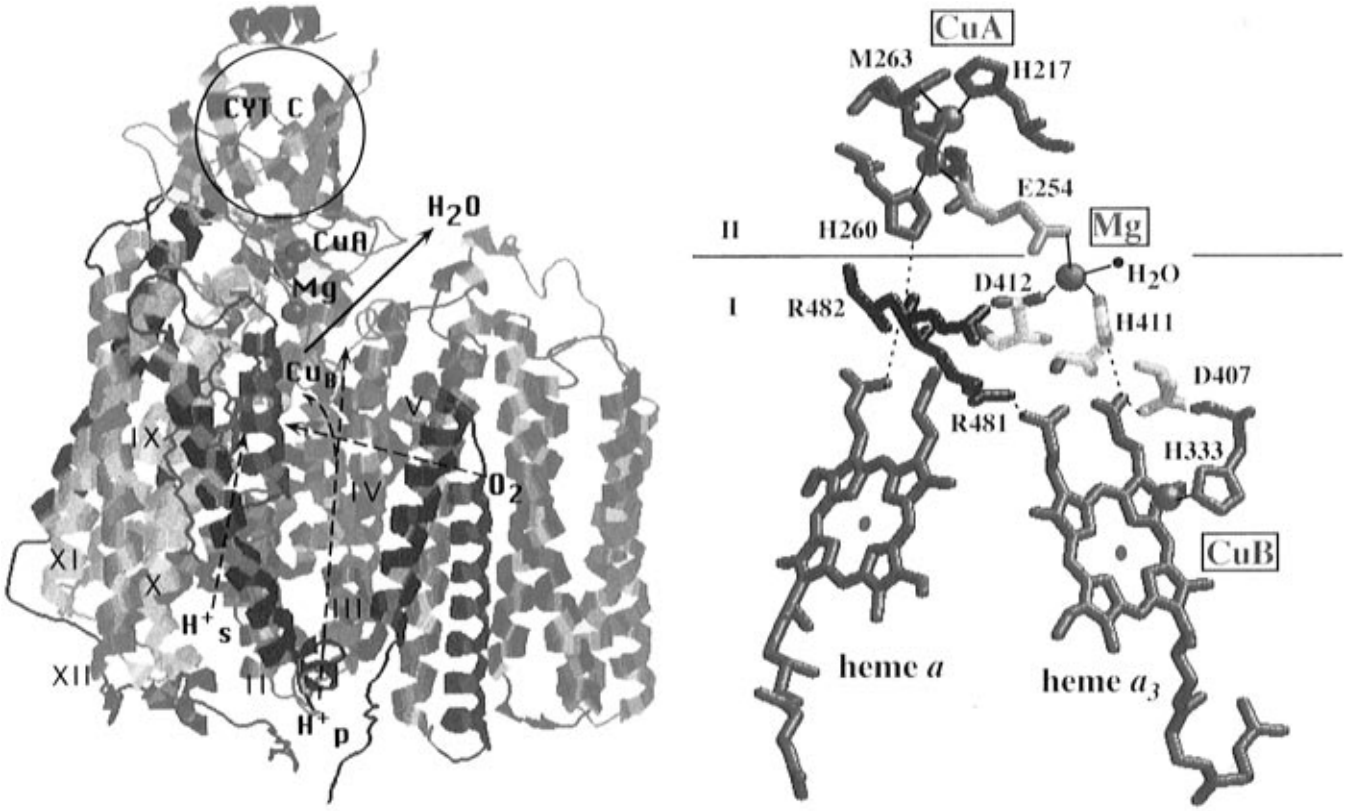

Figure 1. The crystal structure of the three mitochondrially encoded subunits of bovine cytochrome *c* oxidase from the coordinates of Tsukihara *et al.*[12] by generous permission of the authors. (A, left) Overall stucture of the three subunits common to mammalian and bacterial enzymes. The N-terminal of each subunit starts in dark blue and is color-graded through to the C-terminal, which is red in the case of helix XII of subunit I. Some of the helix numbers of subunit I are designated by Roman numerals. Approximate positions of proposed substrate proton (H^+_s) and pumped proton (H^+_p) pathways are indicated in dotted arrows, as well as a proposed O_2 channel. A suggested H_2O channel at the subunit I/II interface is shown with a solid arrow. Heme groups are in red, with only heme *a* substantially visible. A possible location for cytochrome *c* binding is indicated on subunit II. The metal centers are labeled and colored: Mg, red; Cu_A, red; Cu_B, yellow. (B, right) An expanded view of the metal centers and interface region between subunit I and II. Cu_A ligands are green; the shared Cu_A−Mg ligand is dark yellow. Only one of three histidine ligands to Cu_B is shown, in blue. Metal ligand bonds are indicated by solid lines, hydrogen bonds by dotted lines. The residue numbers are for *R. sphaeroides*; corresponding numbers for beef heart and *P. denitrificans* can be found in Table 1. Figures were prepared using Rasmol and Canvas.

One of the most surprising, and reassuring, aspects of the two crystal structures is the essential identity of the metal centers and active site; indeed, the entire three-dimensional structure of the common subunits is highly conserved at an atomic level, to an extent that might not have been expected for such distant relatives as a bacterium and a cow. Figure 1 illustrates the three core subunits of the bovine oxidase[12] and some of the features common to both mammalian and bacterial enzymes. Table 1 gives the corresponding sequence numbers for *Rhodobacter sphaeroides*, *Paracoccus denitrificans*, and bovine oxidases for a number of key residues. In the following section, we discuss the impact of the new structural information on a number of functional issues, including electron entry and transfer pathways, proton exit routes, coupling mechanisms and proton-transfer pathways, predicted water and O_2 channels, and the significance of unique aspects of the mammalian enzyme.

1. Electron-Transfer Pathways

The arrangement of the metal centers and the distance and substance between them is key to understanding the pathway and control of electron transfer. The crystal structures show the metal-center ligands and the positions of the hemes and coppers relative to each other and the membrane to be as indicated by mutant studies and hydropathy plot analysis, although the transmembrane helices are considerably longer, at a greater angle (up to 35° with respect to the vertical to the plane of the membrane), and more kinked than predicted. But the real surprise is the position of the hemes: they are at equal depth in the membrane (13 Å) and perpendicular to the plane of the membrane, but they are not lined up in parallel. Bound to the same helix (helix X in subunit I), with all four propionate side chains pointing toward the outside of the membrane, the heme planes are angled at 104° to each other with their edges 4.5 Å apart at closest approach. Since the iron-to-iron distance is 14 Å, this raises an interesting possibility of edge-to-edge transfer being more efficient than iron to iron. However, the structures do not provide any obvious insight into how electron transfer between heme *a* and a_3 is controlled: the location of the hemes on the same helix precludes any major distance changes, unless edge-to-edge transfer is invoked where slight changes

Table 1. Some Key Residues in Cytochrome *c* Oxidases

function/significance	subunit	helix	residue	residue number in *R. sphaeroides*	*P. denitrificans*	beef heart
metal ligands						
heme *a*	I	X	His	421	413	378
		X	His	102	94	61
heme a_3	I	X	His	419	411	376
Cu_B	I	VI	His	284	276	240
	I	VII	His	333	325	290
	I	VII	His	334	326	291
Cu_A	II		His	217	181	161
	II		His	260	224	204
	II		Cys	252	216	196
	II		Cys	256	220	200
	II		Met	263	227	207
	II		Glu	254	218	198
Mg	I	IX→X	His	411	403	368
	I	IX→X	Asp	412	404	369
	II		Glu	254	218	198
postulated channels						
substrate proton channel	I	VIII	Lys	362	354	319
pumped proton channel						
entry	I	II→III	Asp	132	124	91
exit (Iwata *et al.*)	II	IX→X	Asp	407	399	364
exit (Tsukihara *et al.*)	I	IV	Ser	186	134	142
H_2O channel						
entry	I	(Mg)+	Asp	407	399	364
exit	II		Arg	234	226	178
	I	V→VI	Asp	271	263	227
O_2 channel						
entry	III	(lipid pool)				
exit	I	VI	Glu	286	278	242
postulated electron transfer route						
Cu_A→ heme *a*	II		His	260	224	204
	I	XI→XII	Arg-Arg	481, 482	473, 474	438, 439

in angle or intervening residues might affect the length of a through-space jump. Alternatively, a through-bond pathway postulated between the irons is still tenable in light of the structure and could be controlled by loss of a heme ligand.[19] One such ligand exchange hypothesis (Tyr422 exchanges for His419, a heme a_3 ligand[20]), has been ruled out by mutational analysis of the residues in question.[21] The possibilities of thermodynamic and/or proton-access control are discussed below (section C).

Of particular interest regarding the pathway of electrons in the protein is the location and the dinuclear character of the Cu_A site. The crystal structures show it positioned at the interface of subunits I and II (Figure 1), almost (but not quite) equidistant from the two hemes (19 Å from heme *a*, 22 Å from heme a_3, metal center to metal center). Both structures show a possible covalent- and hydrogen-bonded pathway connecting Cu_A to heme *a* (Figure 1B), which can be argued[10,12,22] to provide a facilitated route for electron transfer to heme *a* to account for the observed high rates.[23−25] The pathway involves the peptide bond between a highly conserved arginine pair (R438,439, bovine; R481,482, *R. sphaeroides*), one of the propionic acid substituents of heme *a*, and a completely conserved histidine ligand to Cu_A (H204 II, bovine; H260, *R. sphaeroides*). However, Yoshikawa and colleagues[12] also point out a similarly conserved, through-bond route to heme a_3 in the mammalian enzyme. Since rapid direct transfer from Cu_A to heme a_3 is not normally observed (though it has been postulated[23]), this leaves unresolved the issue of whether such pathways are critical in control of electron transfer.[26]

The dinuclear character of Cu_A could also play a role in facilitating and directing electron flow. Gray and co-workers[22] calculate an unusually low reorganizational energy favoring rapid electron transfer from Cu_A to heme *a* and suggest that this could be due to the ability of the dinuclear site to delocalize the electron over a large area (see also ref 25 and section E). Indeed, any alteration in the structure of the Cu_A center results in strong inhibition of overall turnover rates of the enzyme.[27,28] But even when the copper site has completely lost its dinuclear character, proton pumping is retained (Zhen, Y.; Mills, D.; Ferguson-Miller, S., unpublished results), indicating that this structure is not required for the pumping function.[29]

2. Proton Exit Routes

The location of Cu_A and a Mg ion at the interface between subunits I and II was foreseen from mu-

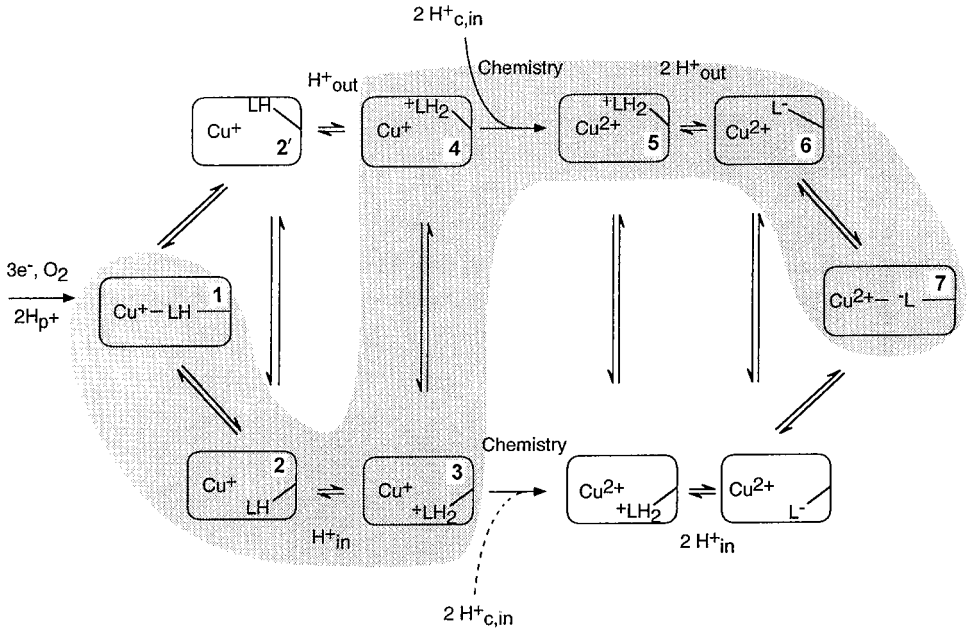

Figure 2. A formulation of the Cu_B−ligand exchange mechanism of proton pumping. The favored proton-pumping pathway is shown in the shaded area. The scheme starts after three electrons and two protons (H^+_p) have been loaded into the heme a_3−Cu_B site (as in refs 10 and 40). In the shaded region, the equilibrium of each reaction is strongly favored in the forward direction, so that LH (histidine in imidazole state) is normally accessible to protons only from the inside (intermediate **2**). When the third proton, H^+_{in}, is loaded (intermediate **3**) to maintain charge neutrality, the equilibrium strongly favors a movement that makes $^+LH_2$ accessible to the outside (intermediate **4**) and opens a channel so that "chemical" (or substrate) protons can access the binuclear center from the inside ($2H^+_{c,in}$) and allow the oxygen chemistry to proceed. The $2H^+_p$ are then released from $^+LH_2$ to the outside (intermediate **5**→**6**) driven by the oxygen chemistry. Insofar as LH can access protons from the outside (through the normal exit pathway) (intermediate **2′**), the reaction is uncoupled and would proceed in the absence of protons from the normal input pathway, as suggested for mutants at D132.[33] Cu = Cu_B; LH = histidine, imidazole; LH_2^+ = histidine, imidazolium; L^- = histidine, imidazolate; H^+_c = chemical or substrate proton; H^+_p = pumped proton; chemistry = oxygen reduction to H_2O. The original version of this scheme was created by Thomas Nilsson, University of Karlstad, Karlstad, Sweden.

tagenesis and spectroscopic studies,[30,31] but the exact position of these metals (Figure 1B) above the binuclear center draws attention to the importance of this region, not only in potentially controlling electron input but also proton output. The I−II interface appears to harbor considerable water and negative charge, leading Michel and colleagues[10] to propose that proton exit would be favored by the charge and hydrophilic character of the region. From the mammalian structure, Yoshikawa and co-workers[12] propose a distinct water channel that is lined by residues from both subunits I and II, as well as the Mg ion that is ligated by a histidine and aspartate from subunit I, a glutamate from subunit II, and at least one water. Since the carboxyl ligand (E254II, *R. sphaeroides*; 198, bovine; 218, *P. denitrificans*) is shared with Cu_A (Figure 1B), Mg is in a critical bridging position between the two subunits and is immediately above the binuclear center (Fe_{a3} to Mg = 15 Å). Is it functionally, as well as structurally, important? If proton pumping is directly coupled to the oxygen chemistry, proton exit would be expected to occur in this area. Insofar as Mg controls the p*K*'s of residues in its vicinity, and/or is an organizing force in a water channel, it could play an important role in regulating proton/water exit and, hence, activity. It is noteworthy that the quinol oxidases, which have neither Cu_A nor Mg, have a distinctively different pH dependence for proton pumping.[32] Mutations that result in loss of Mg show about 50% inhibition of overall activity but no change in proton pumping efficiency.[17,31] However, recent studies on a Mg-ligand mutant in *R. sphaeroides*, His411Gln, indicate a dramatic change in the pH profile of its activity, consistent with a regulatory role for Mg in proton/water exit (Florens, L.; Ferguson-Miller, S., unpublished results). In contrast, mutation of Asp407 in *R. sphaeroides*, also suggested to mediate proton exit,[10] has little effect on proton pumping, activity, or pH dependence of activity, arguing against its importance in structure, function, or regulation (Qian, J.; Ferguson-Miller, S., unpublished results). The position and nature of the proton exit pathway could be critical to understanding the regulation of cytochrome *c* oxidase. Reversal of the exit pathway (e.g. via intermediate 2′ in Figure 2) has been suggested[33] to account for the continued electron-transfer activity of a mutant in which proton uptake from the interior appears to be inhibited and which exhibits "reverse respiratory control".[17] Considering how physiological regulation of efficiency of energy coupling might be accomplished, control of reversal of the exit pathway is an interesting possibility.

3. Electron Entry Sites

Extensive debate has focused on the question of where electrons from cytochrome *c* enter the oxidase and how many docking sites exist. Rapid kinetic techniques have clearly demonstrated that the first center reduced by cytochrome *c* is Cu_A,[23,34] but where cytochrome *c* sits to accomplish this extremely rapid

transfer (>100 000 e^-/s) and whether there is more than one interaction site are not obvious from the structure (but see Figure 1A). However, the structure does provide the opportunity to apply sophisticated docking algorithims (e.g., ref 35) to address this question, which could guide mutational analysis more incisively in the future. Indeed, there are abundant carboxyls in subunit II that could participate in ionic interactions with lysines surrounding the exposed heme edge of cytochrome *c*. Although these charged residues have been demonstrated to play a critical role in the cytochrome *c*/cytochrome oxidase interaction,[36] it is clear that hydrophobic forces may also be important in cytochrome *c* interactions with its redox partners[37,38] and that it is not a trivial pursuit to define such protein−protein interactions even when crystal structures are available.[39]

4. Coupling Mechanisms and Proton Transfer Pathways

The bacterial enzyme structure of Michel and colleagues[10] provided the basis for these authors to refine the model for coupling of oxygen chemistry to proton pumping via ligand exchange of a histidine at the Cu_B site. This model was first proposed by Wikström and co-workers[40] and is indebted to the earlier concept of ligand exchange at the Cu_A site developed by Chan and colleagues.[29] The proposal is consistent with the lack of resolution of one of the histidine ligands (His333, *R. sphaeroides*, Figure 1B) of Cu_B in the structure of the oxidized, azide-inhibited form of *Paracoccus* cytochrome *c* oxidase (although this histidine is resolved in the oxidized mammalian enzyme without azide). As with the original model, the mechanism of Iwata *et al.*[10] demands separate access to the active site of protons to be pumped and substrate protons destined to make water and invokes the principle of strict maintenance of charge neutrality[41] by uptake of protons to neutralize electron transfer to the heme a_3−Cu_B center. Thus, the driving force for proton uptake is charge neutralization, while the gating of the proton channel is provided by the movement of the histidine from Cu_B after it is doubly protonated to the imidazolium form. In Figure 2, some elements of the gating/pumping function are illustrated in a more specific way, drawing attention to the potential reversibility of steps in the sequence and suggesting the concept of a gate (the movement of the histidine ligand) that not only changes the access of protons to be pumped from one side of the membrane to the other but at the same time allows access of substrate protons to the active site so that the oxygen chemistry can proceed. The histidine shuttle model has many attractive features and provides a concrete, testable theory for future investigation. But the crystal structures pose a problem regarding the issue of charge neutrality: no bridging or neutralizing ligand is resolved between the positively charged Fe_{a3} and Cu_B, which are 5 Å apart. The structure rules out any of the amino acid side chains in the vicinity as bridging ligands, but at the current 2.8 Å resolution, the presence of a somewhat disordered exogenous ligand cannot be dismissed.[119−121]

The substrate proton channel is visualized in both crystal structures as a direct route to the heme a_3-Cu_B center involving residues of helix VI and helix VIII. Mutation of a lysine in helix VIII (K362, *R. sphaeroides*; 354, *P. denitrificans*; 319, bovine) demonstrated that replacement of this residue causes complete inactivation of the enzyme in spite of minimal alteration of the spectral properties of the active site.[42,43] However, another characteristic, very slow reduction of heme a_3 in these mutants,[43] would appear to be inconsistent with the pumping model of Iwata and colleagues,[10] in which uptake of protons from the pumping pathway, not the substrate pathway, neutralize the first three electrons entering the binuclear center.

An input channel for pumped protons is identified in the bacterial enzyme based on results of mutational analysis of cytochrome aa_3[17] and bo_3,[16,18] which reveals a critical aspartate residue between helix II and III (D132, *R. sphaeroides* aa_3; D135, *Escherichia coli* bo_3) the replacement of which results in loss of proton pumping but retention of some electron-transfer capacity. A possible hydrogen-bonded pathway for proton movement is traced in the bacterial crystal structure leading toward the a_3−Cu_B site and a conserved glutamate in helix VI (E286, *R. sphaeroides*; 278, *P. denitrificans*; 242, bovine). But the route is not complete, possibly because potentially important water molecules are not resolved.

More water is defined in the mammalian enzyme structure, and two different pathways for pumped protons are suggested. Although one pathway starts at the same aspartate as in the bacterial enzyme (Figure 1A), neither follows the same route proposed by Iwata and co-workers, nor does either access the a_3−Cu_B center. On this basis, Tsukihara and colleagues suggest an indirect, conformationally coupled proton pump rather than direct coupling to the oxygen chemistry.[12]

5. Water and Oxygen Channels

One of the suggested pumping pathways, involving helices III and IV,[12] ends at the proposed water channel (see Figure 1A), raising the interesting question of whether proton exit accompanies water extrusion. It is noteworthy that, at the turnover rate of 2000 electrons per second observed in bacterial enzymes, 1000 waters will be produced per second and must be extruded from the active site. The water channel suggested in the mammalian X-ray structure[12] is similar to the hydrophilic cleft observed in the bacterial enzyme proceeding from the binuclear center to the outside of the membrane. It is lined by a number of hydrophilic residues from both subunits I and II, as well as the Mg binding site. The existence and significance of this channel remains to be established, but it is reasonable to consider a possible additional role in proton exit, which must proceed at double the rate of water if the system is fully coupled.

Along with the necessity of getting water and protons out of the active site, oxygen must be brought in. Since oxygen is an order of magnitude more soluble in organic than aqueous solvents, entry of O_2

to the active site would be expected to take advantage of higher O_2 concentrations in the membrane and facilitate diffusion through hydrophobic regions of the protein. In the mammalian enzyme, three possible O_2 channels are suggested, each of which has significant hydrophobic character and accesses the membrane phase. An intriguing structural feature in both enzymes is the existence of a trapped lipid pocket in subunit III and a putative O_2 pathway leading directly from this pocket to the active site (Figure 1A). In fact, a "hole" in the space-filling model of the coordinates allows a residue close to Cu_B (E286, *R. sphaeroides*; 278, *P. denitrificans*; 242, bovine) to be seen from the surface. This channel would appear to have the advantage of a built-in oxygen reservoir, even though the two other possible channels have shorter paths to the bulk membrane phase. It could be argued, of course, that a facilitated oxygen channel is unnecessary, since oxygen concentrations are normally far in excess of the O_2 affinity of the enzyme, so access of O_2 would not be rate limiting. However, recent mutational efforts to block the putative O_2 channel from the subunit III pocket provide good support for a rate-limiting, favored access route.[115]

6. Unique Aspects of the Mammalian Oxidase Structure

The mammalian enzyme, though retaining the highly conserved three-subunit core and essentially identical metal site structures, has 10 additional peptides, the locations of which are now identified in the crystal structure. But knowing their structure and position does not solve the mystery of their functional or regulatory significance. None of the nuclear encoded subunits is closely associated with the active site, suggesting that the additional peptides have not taken over any mechanistically important functions. It is obvious to suggest a stabilizing and insulating role, given the longer life of the eukaryotic enzyme (days instead of hours) and the need to protect against release of damaging radical intermediates. However, it is well established that some of the subunits are tissue and developmentally specific, suggesting a regulatory function in the more complex eukaryotic systems.[44] Indeed, several (VIa,b,c) are in contact with the region above the binuclear center where cytochrome *c* binds and protons and water are likely extruded. In this location they could impact on electron input and proton or water output, and thus influence the activity and efficiency of the enzyme. Similarly, peptides on the inner surface (e.g., Vb, which binds a zinc ion) could affect proton uptake.

Another interesting revelation from the crystals[12] is the location of two possible nucleotide binding sites, occupied by a detergent analogue, cholic acid. A number of previous studies have demonstrated binding of ATP to eukaryotic cytochrome *c* oxidase and regulatory effects on oxidase activity and proton pumping.[45,116] The structure adds substance to this regulatory possibility and implies an allosteric effect, but until the electron-transfer and pumping processes are clarified, regulatory mechanisms will be difficult to decipher.

The dimer state of the bovine oxidase found in the crystal form is intriguing: there is very little protein:protein contact, the interaction being mediated by only two small subunits VIa and VIb. The two monomers capture a lipid pool between them—large enough to hold two cardiolipin molecules but these have not yet been resolved. Tsukihara *et al.*[12] argue for functional significance to this dimer structure, but convincing evidence for more than a stabilizing role has yet to be obtained.[46]

C. Bioactivation and Reduction of Dioxygen

We now turn from the structural considerations above to mechanistic aspects of oxidase function. We begin with general features of oxygen activation and then focus attention on oxidase catalysis specifically. The reduction of dioxygen to water is a chemically complex process. Electron addition, protonation, and O═O bond cleavage must occur, and, necessarily, we expect intermediate species in this process. We can represent this sequence of events in a schematic way, as follows:

$$O_2 \xrightarrow[e^-]{} [I] \xrightarrow[H^+]{} H_2O, \text{ products}$$

where [I] represents intermediate species in the process. This representation is, of course, an oversimplification, as four electrons and four protons are involved in the reaction; but, for the general discussion that follows, the above provides a useful framework within which to consider mechanistic aspects of dioxygen reduction.

1. Oxygen Toxicity and Electron-Transfer Control

Owing to the high reduction potential of dioxygen, the partially reduced intermediate species, which may include superoxide, peroxide, and hydroxyl radical, depending on the specifics of the reduction pathway, are themselves highly oxidizing and potentially toxic in a biological milieu. As a consequence, we expect that control mechanisms have evolved in enzymes that metabolize dioxygen to minimize spurious chemistry involving these species that would be deleterious to the cell. One such control mechanism can be envisioned that involves making electron input in the scheme above the overall rate-limiting step in the reduction process. In this scenario, the protonation events would be fast and the transient buildup of intermediate concentration would be minimized. Operationally, this electron-transfer control mechanism may involve preloading the enzyme-active site with protons so that diffusional delays in proton delivery are eliminated.

The cytochrome P450 class of enzymes provides an excellent example of electron-transfer control. Figure 3 shows a postulated mechanism for oxygen activation and substrate hydroxylation by P450.[47] Beginning with the ferric enzyme, substrate (SH) binds and one-electron reduction produces the ferrous high-spin form of the enzyme. Oxygen binds to this species and, in the overall rate-limiting step in the reaction, electron injection from an external reductant initiates

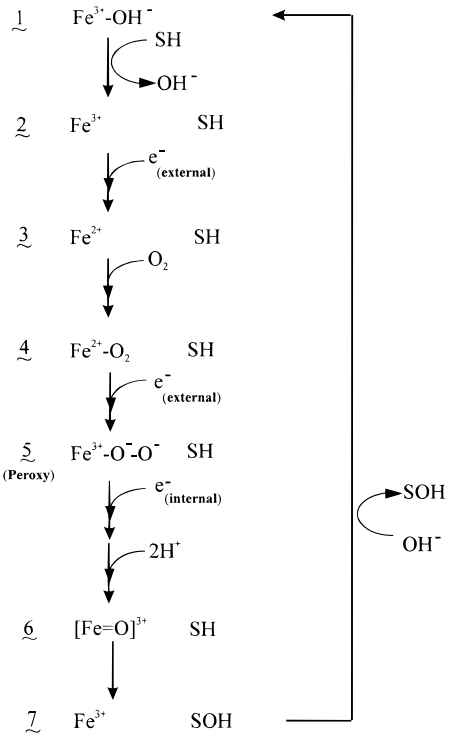

Figure 3. Postulated P450 reaction cycle; SH represents substrate, which is bound into the active site and hydroxylated to product SOH.

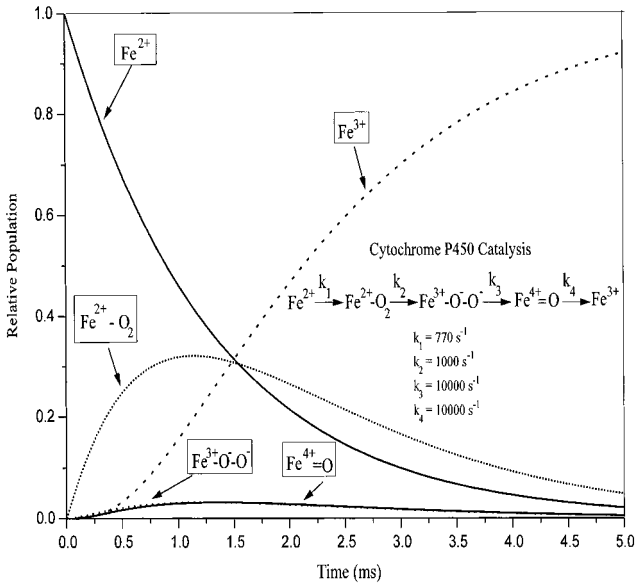

Figure 4. Concentration *versus* time profiles for various intermediates in the P450 reaction cycle with mechanism and rates as indicated.

catalysis. Subsequent steps, which, presumably, proceed through peroxy and ferryl intermediates, the latter of which is thought to be the actual hydroxylating intermediate, are fast; product (SOH) release regenerates the oxidized enzyme. Figure 4 shows a simulation of the transient concentrations of the various species in the P450 reaction mechanism.[48] The rate constants used in the simulation for the various steps are consistent with data in the literature; the rate-limiting electron injection is taken to be at least 10 times slower than other steps in the process. As is clear in the simulation, only the ferric, ferrous, and ferrous oxy species occur at appreciable concentration during turnover; in particular, the concentrations of the reactive, and potentially cytotoxic, peroxy and ferryl intermediates are minimized.

2. Proton-Transfer Control and the Proton Pump in Heme/Copper Terminal Oxidases

A second means by which the dioxygen chemistry in the scheme above could be controlled is by transferring the rate limitation to the protonation step. At first glance, this appears to be a poor strategy, *vis-a-vis* toxicity, as this type of control mandates that the reaction decelerates as it proceeds, i.e., successive steps slow down, relative to preceding reactions in the mechanism. This contrasts sharply with the acceleration that characterizes electron-transfer control. As a consequence, intermediates build up and persist during turnover.

Recent work on the non-heme enzyme methane monooxygenase (MMO), which activates dioxygen and inserts a single oxygen into a C−H bond in methane to produce methanol, had indicated that this enzyme follows a proton-transfer type control mechanism, that is, the reaction with oxygen slows down as it proceeds.[49−51] Under these conditions, a wealth of kinetic and spectroscopic information on the intermediate species is accessible and has been obtained. This behavior had been puzzling, however, in terms of the considerations above, as it suggests that MMO should be susceptible to damage from intermediates that accumulate. Recent work from Lipscomb's lab has clarified this paradox, as it indicates that, when the MMO hydroxylase component is reconstituted with both its reductase and a third protein component, B, the concentration of transient intermediates under turnover conditions drops significantly (ref 52 and Lipscomb, J. D., personal communication). This observation suggests that, although the isolated hydroxylase component apparently follows a decelerating kinetic scheme characteristic of proton involvement in rate-limiting steps, the more native reconstituted system shifts to what appears to be an electron-transfer limited mechanism. The recent observations on the P450 and MMO systems provide confidence in the above analysis of modes of control in oxygen-metabolizing enzymes—a critical issue appears to be minimizing the concentration of potentially toxic, dioxygen-derived intermediates during catalysis.

Despite this generalization, time-resolved optical and resonance Raman work on the reduction of dioxygen by cytochrome oxidase clearly shows that the kinetics of this process exhibits the hallmarks of proton-transfer control: the reaction decelerates as it proceeds, transient intermediates build to detectable concentrations, and pH dependencies are clearly apparent in the later stages of the reaction. Figure 5 shows a typical simulation of time/concentration profiles for cytochrome oxidase during its reaction with O_2 from a series of time-resolved resonance Raman measurements.[53] Although the details of the postulated mechanism are under debate (see below), there is consensus on the generalization that inter-

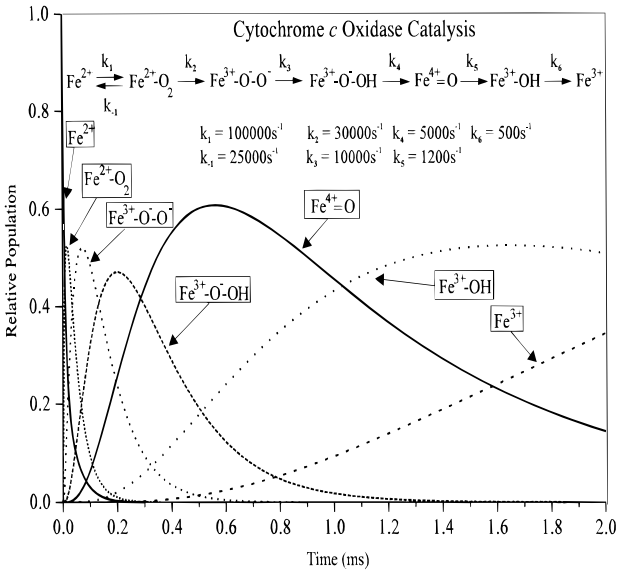

Figure 5. Concentration *versus* time profiles for various intermediates in the fully reduced cytochrome oxidase/dioxygen reaction. Rates and postulated mechanisms are taken from refs 53 and 74.

mediate species in the reduction process accumulate to considerable levels.

The physiological basis for this unexpected behavior can be rationalized within the context of the proton-pumping function of the enzyme and the necessity of maintaining tight coupling between the electron transfers to the partially reduced oxygen intermediates that drive the pump and the molecular machinery in cytochrome oxidase that carries out the pumping function. Figure 6 shows a simplified scheme of the catalytic cycle in the cytochrome oxidases. Reduction of the binuclear site in the enzyme produces the ferrous/cuprous form of the protein. Dioxygen binding generates the oxy intermediate (see below), which then undergoes successive conversion to peroxy, ferryl, and hydroxy intermediates. Only the late intermediates, the peroxy and the ferryl, in this process are sufficiently oxidizing to drive proton translocation, and Wikström has shown experimentally that it is, indeed, the reduction of these two species that is coupled to the pump.[54] By transferring control of these two reduction processes to protonation, rather than electron transfer, reactions, tight coupling between the proton-pumping action and the electron transfer that drives it can be maintained. In essence, proton-transfer control allows protons to be loaded into proton-pumping sites prior to the delivery of substrate protons and electrons to the oxygen intermediate for which the reduction drives the pump. Thus, a physiological rationale for the unusual, decelerating, proton-transfer-controlled kinetic mechanism used by cytochrome oxidase in dioxygen reduction can be developed.[3,48,55]

The proton controls operating in cytochrome oxidase have a number of important implications. First, as indicated above, intermediates in the process develop to substantial concentrations. This provides an opportunity to characterize them structurally, and considerable progress has been made on this, as described below. Second, the occurrence of relatively long-lived, potentially toxic intermediates in O_2 reduction suggests that the protein has devised either sequestering mechanisms to shield them from deleterious side reactions or that the reactivity is controlled by carefully orchestrated proton deliveries to oxy species that are relatively unreactive in the absence of H^+. In some aspects, this situation resembles the "negative catalysis" concepts that Rétey has developed for the chemistry in amino acid radical based enzymes.[56] The key idea he has put

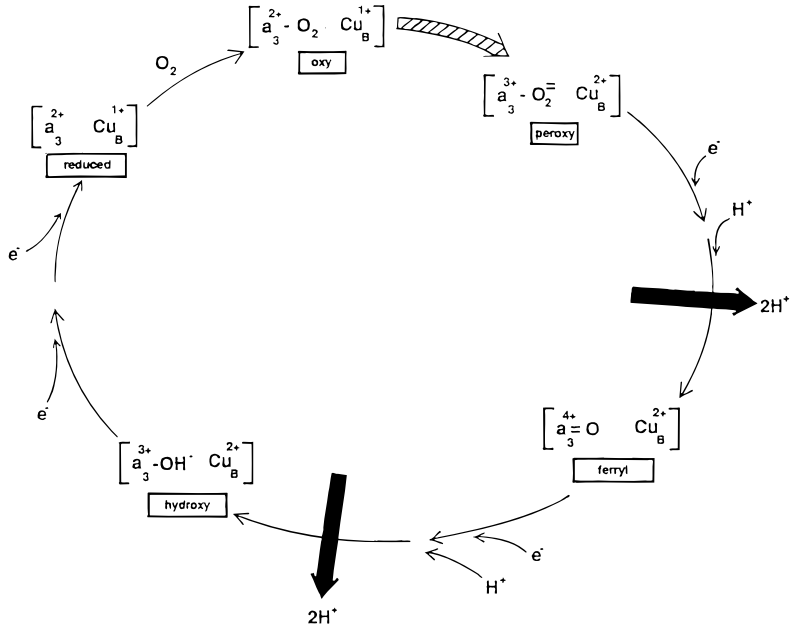

Figure 6. Simplified reaction scheme for oxidation of reduced cytochrome oxidase by dioxygen. The reduced binuclear center reacts with O_2 to form an oxy intermediate, which undergoes successive one-electron reductions to form peroxy and ferryl intermediates, respectively. These latter two electron transfers are coupled to proton translocation, as indicated by the heavy, shaded arrows. The structures of the intermediates are used only for an electron count and are not intended, necessarily, to represent actual, proposed structures.

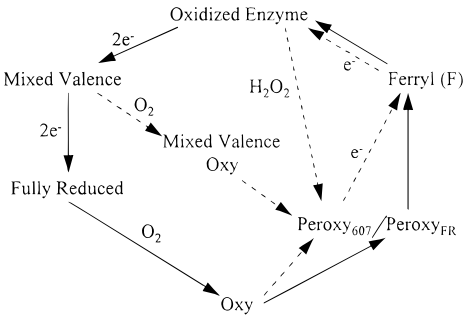

Figure 7. Reaction sequences schematizing reaction of cytochrome oxidase in its fully reduced and mixed-valence states with dioxygen and in its oxidized state with H_2O_2. The solid arrows show the four-electron reduction of the oxidized enzyme and the subsequent reaction of the fully reduced protein with O_2. The peroxy intermediate on this pathway is designated "$Peroxy_{FR}$" (see the text). The reaction of the mixed-valence enzyme with O_2 and of the oxidized enzyme with H_2O_2 is shown by the dashed arrows to produce the peroxy species designated "$Peroxy_{607}$" (see the text). One-electron reduction of this species produces the ferryl along the dashed arrow, which can be one-electron reduced, in turn, to form the oxidized enzyme.

forward is that, with the generation of the radical species, energetic barriers to reactivity have been overcome and the function of the protein is simply to direct this reactivity to the appropriate substrate, while minimizing spurious side reactions. In oxidase, with the generation of peroxy and ferryl species, an analogous condition occurs. Clearly, access limitation appears to be the case in the protein, as the binuclear center is deeply buried in the protein (Figure 1). Mechanistic proposals for the proton pump (Figure 2 and below) also invoke carefully timed proton delivery as a central theme.

With this general description of dioxygen reduction mechanisms, we now turn to specific aspects of the oxidase/O_2 reaction and its coupling to the proton pump.

D. Reaction of Cytochrome Oxidase with Oxygen-Containing Substrates

A variety of biochemical and spectroscopic methods have been used to investigate the chemistry that occurs when cytochrome oxidase reacts with dioxygen or with its partially reduced redox intermediates. The enzyme shows a wide range of reactivities and, accordingly, a range of reaction conditions has been employed. Thus, for example, the fully reduced enzyme can be studied in its reaction with dioxygen and the fully oxidized protein can be induced to react with hydrogen peroxide. The latter reaction is complicated by the fact that peroxide can act as both oxidizing and reducing substrates for cytochrome oxidase. Nonetheless, this chemistry can be sorted out reasonably well. Interestingly, common intermediates are observed in these various reactions and have provided the underlying motivation for their study. The basic framework within which these reactions have been interpreted is presented in Figure 7. The fully oxidized enzyme can be reduced by two electrons in the presence of CO to produce the mixed-valence species in which the binuclear center is reduced and the *a* and Cu_A sites remain oxidized. Further reduction produces the fully reduced protein. As noted above, reaction of either the mixed-valence or fully reduced proteins with O_2 produces an oxy species in which dioxygen is ligated to the iron of heme a_3. In subsequent steps, the oxy relaxes through species that are formally at the peroxy redox level (see below) and then to a heme a_3 ferryl intermediate before reforming the fully oxidized enzyme. Reaction of fully oxidized cytochrome oxidase with hydrogen peroxide produces a formal peroxy species directly, which then can be reduced to a ferryl; ultimately the oxidized protein is regenerated. Although the overall reaction cycle for the reaction of cytochrome oxidase with dioxygen can be sketched in broad outline, the details of the process and its control are the subjects of intense activity and debate. In the subsections that follow, the major current issues are considered and discussed.

1. Dioxygen Binding and the Initial Oxy Intermediate

A range of spectroscopies has established that the initial dioxygen complex at the binuclear center resembles the oxy complexes of myoglobin and hemoglobin. A key element in these studies has been the use of the carbon monoxide complex of the binuclear center as the initial reactant in the oxygen-binding process. As with other hemes, the CO complex is photolabile, and photolysis of this ligand in the presence of O_2 can be used to initiate O_2 binding so that time-resolution restrictions imposed by mechanical mixing processes are circumvented.[57,58] The kinetic constants for CO ligation and dissociation and O_2 binding for cytochrome oxidase are such that essentially complete conversion from the carbon monoxy complex to the oxy complex can be achieved on a single photolysis pulse. This set of kinetic constants, particularly the slow CO association rate constant, is unique among heme proteins, and only with oxidase can the conversion of carbon monoxy to oxy be achieved with such effectiveness.[3]

Gibson and Greenwood developed the CO photolysis methods and showed that the reaction with dioxygen occurs on the microsecond time scale when O_2-saturated buffer is used.[58] The initial binding reaction, however, shows saturation kinetics, which suggests oxygen binding in the enzyme at a site that precedes binding to the heme. This idea was strengthened by the observation that CO ligates transiently at Cu_B following its photodissociation, which implicated ligand binding to this metal as the likely explanation for the dioxygen kinetic behavior.[59,60] Blackmore *et al.*[61] and Woodruff and co-workers[5,62−65] have expanded considerably the data base supporting O_2 association with Cu_B^{1+} prior to binding at the heme.

The buildup of a discrete oxy intermediate during catalysis was initially proposed by Chance and co-workers in low-temperature EPR−trapping experiments[66,67] supported by time-resolved optical measurements in the visible region[68,69] and by time-resolved Raman experiments in the high-frequency vibrational region[70] and demonstrated with the latter

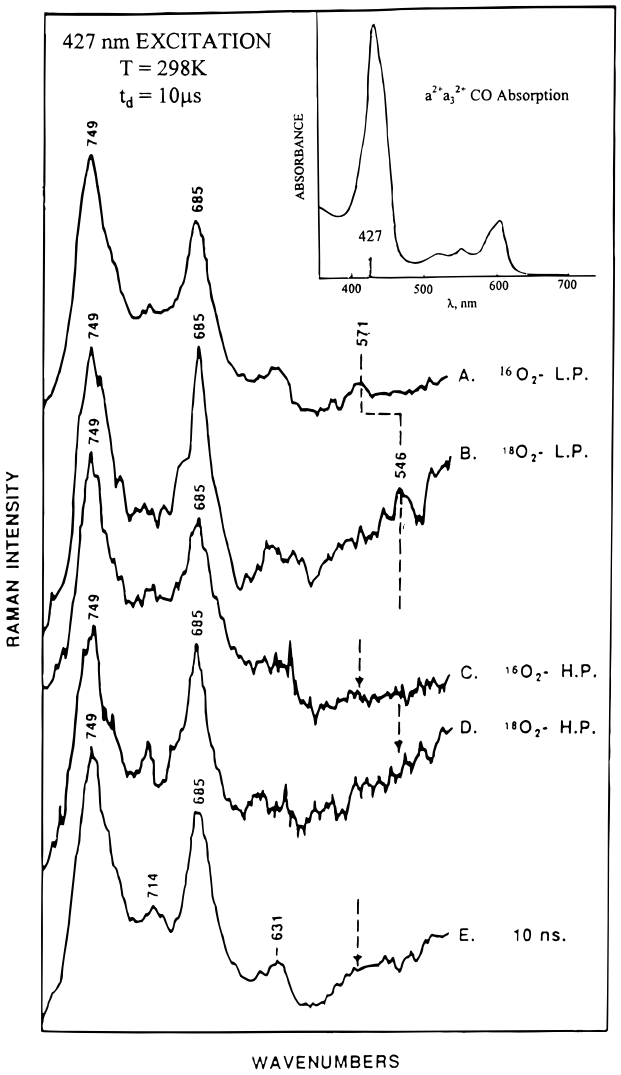

Figure 8. Resonance Raman spectra recorded at 10 μs following the initiation of the reaction between reduced cytochrome oxidase and O_2. The mode at 571 cm^{-1} in A, recorded with $^{16}O_2$, shifts to 546 cm^{-1} when $^{18}O_2$ is used as the substrate (spectrum B). Traces C and D show that the oxy intermediate detected is photolabile. See ref 71 for details.

technique by direct observation of the $^{16}O_2/^{18}O_2$ isotope shift for a mode that occurs at 572 cm^{-1} with the natural isotope abundance ligand[71−73] (Figure 8). The 572 cm^{-1} mode arises from the Fe−O_2 stretch and is formed within 5 μs of initiating the reaction with the fully reduced or the mixed-valence enzyme in O_2-saturated buffer.[74] The ν(Fe−O_2) stretching vibration in oxy cytochrome oxidase is similar to the ν(Fe−O_2) frequency in oxy hemoglobin or oxy myoglobin and can be reproduced well with six-coordinate oxy heme *A* model compounds.[75] This indicates that the initial reaction product with O_2 at heme a_3 binds in a relaxed, end-on configuration; there is no apparent interaction with Cu_B in the oxy heme a_3 species.

2. The Decay of the Oxy Species and the Peroxide Issue

The decay of the oxy adduct of heme a_3 signals the onset of the electron and proton transfer processes that couple oxygen reduction chemistry to proton translocation. At present, the oxy decay and the sequence of intermediates that occur at the formal peroxide level of substrate O_2 reduction are the least well resolved, and considerable research effort is aimed at elucidating the processes that occur as the enzyme passes into and out of the formal peroxide level. Issues that are under active scrutiny at present include the following: (a) the electron source in the decay of the oxy to the peroxy oxidation state; (b) the timing of the dioxygen bond cleavage chemistry and the structure of the peroxy intermediate; (c) the role of protons in promoting processes at the peroxy level; and (d) the relevance of the 607 nm absorbing species, which has been assigned to a peroxy intermediate, to the reaction of the fully reduced enzyme with O_2.

The lifetime of the oxy species depends on the valence state of the enzyme: in the mixed-valence species, the oxy intermediate decays with a rate of 5 × 10^3 s^{-1};[68,76] in the fully reduced enzyme, the decay occurs with an apparent rate constant of 3 × 10^4 s^{-1}.[3,23,74,77−80] In neither the mixed-valence nor the fully reduced enzyme is the nature of the state into which the oxy decays well understood. For the mixed-valence enzyme, the ultimate product, first identified by Chance and co-workers as compound **C**, has an absorbance difference spectrum relative to the resting enzyme with an absorbance maximum at 610 nm and Soret absorbance at 428 nm.[66,68] A similar red-shifted absorber, although with an absorbance maximum at 607 nm, is observed in the reaction of the oxidized enzyme with peroxide[81−83] and in "reversed flow" experiments with the fully oxidized enzyme.[84] In both species, as well as in the reaction of the mixed-valence enzyme with O_2, the binuclear center is formally at the peroxide oxidation level and, accordingly, these species are commonly referred to as "peroxy" intermediates.[85] Significantly, its formation in the reaction of the mixed-valence enzyme with O_2 is not accompanied by the uptake of protons from the bulk solution.[86] We will return, below, to a further discussion of "peroxy" species formed in these partial reactions.

The fate of the oxy intermediate in the reaction of the fully reduced protein with O_2 contrasts sharply with that of the mixed-valence enzyme. The reaction proceeds at 3 × 10^4 s^{-1}, roughly 6 times faster than the decay of the oxy in the mixed-valence reaction; both Raman and optical spectroscopies are consistent in showing that the decay of the oxy species corresponds to the oxidation of the low-spin heme *a* center.[3,23,77,78,117] The process is independent of pH, although the Göteborg group has shown that there is a deuterium isotope effect for the coupled oxy decay/a^{2+} oxidation process that suggests internal proton motion as the electron moves from a^{2+} to the binuclear center.[87] Thus, the overall valence of the binuclear center following the decay of the oxy is a function of whether the fully reduced or mixed-valence enzyme is used as the initial reactant: in the mixed-valence enzyme, we can represent the binuclear site following oxy decay at 5 × 10^3 s^{-1} as a_3^{3+}/O_2^{2-}/Cu_B^{2+}, where the notation is used only to count electrons; in the reaction of the fully reduced enzyme,

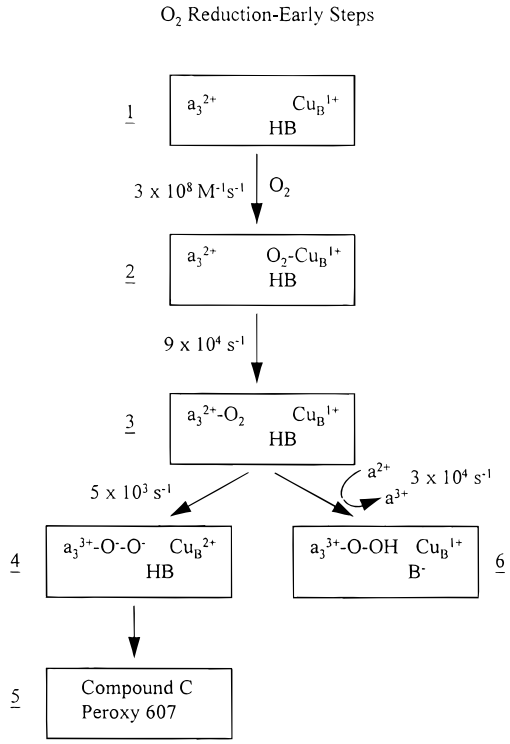

Figure 9. The initial stages in the reaction of the mixed-valence and fully reduced enzyme with O_2. B represents a base function in the binuclear site that can be protonated (HB) or deprotonated (B^-). Apparent rate constants for individual steps are indicated and each of the reaction intermediates is indicated by number as it appears in the sequence.

the oxy species decays with the delivery of the third electron to the binuclear center at a rate of 3×10^4 s^{-1}; in the electron-counting representation, we can schematize the binuclear center as $a_3^{3+}/O_2^{2-}/Cu_B^{1+}$. Thus, there is an additional electron present in the binuclear center, following the decay of the oxy species in the fully reduced enzyme (see Figure 9).

The dependence of the kinetics and mechanism of the oxy decay on the overall valence of the enzyme is a surprising observation that may reflect the onset of proton control in the reduction of dioxygen. Rich and his co-workers have shown that proton uptake accompanies reduction of the binuclear center;[41,88,89] the structure of the enzyme suggests that histidines in the coordination environment of Cu_B may participate in these protonation reactions.[10−12] In the fully reduced enzyme, the protons that were taken up during the reduction phase are likely to facilitate the oxidation of heme a^{2+} that promotes oxy decay. Hallên and Nilsson have shown that the 3×10^4 s^{-1} rate that is observed for the coupled heme a^{2+} oxidation/oxy decay, while pH independent, shows a deuterium isotope effect of 1.4.[87] They interpreted the isotope effect to indicate that electron transfer from a^{2+} into the binuclear center is accompanied by proton motion to the nascent peroxy species. Although analogous isotope effect experiments have not been carried out for the decay of the oxy species in the mixed-valence enzyme, proton motion to trap the peroxy may not occur efficiently in the partially reduced enzyme. Thus, intramolecular proton motions may provide a rationale for the different decay route followed by the initial oxy species.

Figure 9 summarizes the above considerations by showing the initial steps in the binding and reduction of dioxygen in the mixed-valence and fully reduced enzymes. Substrate O_2 binds initially at Cu_B^{1+} and is transferred intramolecularly to the ferrous a_3 site; with saturating O_2 concentrations, the oxy is formed within 5 μs in both the fully reduced and mixed-valence enzymes. The base functionality is represented as HB; protonation of this group occurred as the binuclear center was reduced. In the fully reduced enzyme, electron transfer from a^{2+} is stabilized by coupled protonation of the peroxy; the initial product of oxy decay is the monoprotonated peroxy coordinated to a_3^{3+} and Cu_B remains in its cuprous state. The initial peroxy species is photolabile in that the electron transfer to form the $a^{3+}/a_3^{3+}-O^--OH$ species can be photoreversed.[90] Raman scattering from this species, however, has not been observed. In the mixed-valence species, proton motion to trap the peroxy is suggested to be retarded or absent, and the decay of the oxy is correspondingly slower. Nonetheless, oxidation of Cu_B does occur and this pathway ultimately produces the 607 nm absorbing peroxy species. We suggest, in agreement with the initial proposal by Han *et al.*,[77] that the decay of the oxy by the Cu_B^{1+} oxidation pathway is operative in the fully reduced enzyme with the same 5×10^3 s^{-1} rate constant that characterizes the mixed-valence enzyme. Thus, even in the reaction of the fully reduced enzyme with O_2, we suggest that there will be a branch at the oxy species and that the product distribution will be determined by the rate constant ratios, i.e., that about 85% of the reaction proceeds through the $a_3^{3+} - OOH/Cu_B^{1+}$ species and the remainder through the $a_3^{3+} - OO^-/Cu_B^{2+}$ pathway.

3. The Peroxy and Ferryl Levels in the Reduced-Enzyme/O_2 Reaction

Formation of **5** in Figure 9 is not accompanied by proton uptake; presumably the two protonation processes that occur during reduction of the binuclear center provide the protons necessary either to maintain electroneutrality or to minimize electrostatic effects. The actual oxygen structures in the binuclear center along the compound **C** pathway are uncertain at present; we defer this issue and focus now on processes that occur following formation of the initial peroxy species (**6** in Figure 9) in the fully reduced enzyme.

Optical spectroscopy has been used extensively to follow the kinetics of the later steps in O_2 reduction by the fully reduced enzyme. Following the proton-coupled oxidation of a^{2+}, electron equilibration between the a^{3+}/Cu_A^{1+} sites occurs and is detected as a restoration of absorbance in the 440 nm region of the optical spectrum.[23,79,80,87,91] The rate for this reaction is pH dependent and has a limiting value at low pH of 10^4 s^{-1}. Optical measurements of proton uptake show that protons are taken up from solution with the same rate constant and that the pH dependency of the H^+ uptake process follows that of the a^{3+}/Cu_A^{1+} equilibration; moreover, both the proton uptake and

the electron redistribution show deuterium kinetic isotope effects of 1.4.[87] These observations suggest clearly that the two processes are linked mechanistically. Oliveberg and Malmström rationalized this linkage by suggesting that protonation at the binuclear center triggered electron transfer from Cu_B^{1+} to the ferric peroxy species in **6**; oxidation of Cu_B drove heme a^{3+} to its high potential form, owing to the anticooperative redox interaction between these two centers,[2] and allows electron equilibration between a/Cu_A to occur.[92] Blair *et al.* had suggested a ferrous cupric peroxide earlier from their low-temperature EPR measurements on frozen−trapped intermediates.[93] Overall, the decay of **6** and the electron redistribution between the a/Cu_A sites represents an excellent example of proton-controlled processes in the oxidase/O_2 reaction.

The final kinetic phase detected optically in the fully reduced protein/O_2 reaction is an order of magnitude slower than that that triggers ferrous/cupric/peroxy formation.[58,69,87,91] The reaction shows a strong pH dependency and a deuterium kinetic isotopic effect of 2.5; moreover, proton uptake measurements show that a proton is taken up from bulk phase with the same rate constant and the same pH dependence.[87] The Gotebörg group has characterized this process in some detail and has shown that this phase corresponds to the injection of the final electron from a^{2+}, which was regenerated in the previous kinetic step,[23] into the binuclear center. Proton control is evident, and there are additional aspects to this process that indicate that it is more complex than one would infer from the relatively straightforward exponential kinetics. The 10-fold delay in time in the appearance of this phase, relative to the preceding optically detected process, suggests that there is substantial reorganization in the binuclear center that is not accompanied by significant Soret absorbance changes. Moreover, the proton uptake process is not stoichiometric with enzyme concentrations,[87] which suggests that the observed extent of proton disappearance from solution reflects the sum of both uptake and release processes. These protonation/deprotonation processes may be driven by substrate chemistry, proton-pumping activities, and Bohr effect processes. We have, at present, only a glimpse of the complexity of the processes that occur in the enzyme during the hundreds of microseconds kinetic processes—the summary of intermediates given in Figure 7 is clearly only a skeletal view of the underlying mechanism.

While optical spectroscopy has been incisive in delineating the kinetics of both proton and electron movements, it has been less useful in providing insights into the structures of the partially metabolized oxygen intermediates. Raman spectroscopy has the potential to be more informative structurally and has been applied extensively in time-resolved approaches in the various reactions between cytochrome oxidase and dioxygen (for reviews, see refs 6 and 48). In addition to the oxy intermediate noted above, Raman has detected four other oxygen-isotope-sensitive vibrations under diverse conditions. Table 2 summarizes the modes observed, their isotope sensitivities, the conditions under which each is observed, and postulated assignments by the three different groups who have carried out the Raman measurements.

In terms of reactions at the peroxy and ferryl levels in the fully reduced enzyme/O_2 reaction, three modes are relevant, those at 356, 785, and 804 cm^{-1}. Of the three modes mentioned, there appears to be emerging consensus that the 785 cm^{-1} mode, which has been conclusively assigned as Fe^{IV}=O by both Varotsis *et al.*[74] and Ogura *et al.*[95] in $^{16}O-^{18}O$ mixed-isotope experiments, comes relatively late in the reaction and is preceded by the 356 cm^{-1} and, when observed, the 804 cm^{-1} mode. The 785 cm^{-1} species most likely reflects the ferryl species that is usually referred to as "F" in simplified versions of the reaction sequence (see Figure 7 above), i.e., the species the reduction of which is coupled to the translocation of the second of the two pairs of protons through the enzyme. This species shows unusual behavior, however, in D_2O, as indicated in Table 1. Both Han *et al.*[99] and Varotsis *et al.*[74] noted that the 785 cm^{-1} species apparently shifted up by 10−15 cm^{-1} in D_2O, and they reached the straightforward, but surprising, conclusion that the 785 cm^{-1} ferryl is hydrogen bonded and that the upshift resulted from deuterium exchange into the hydrogen bond. Kitagawa and co-workers have suggested, alternatively, that the H_2O/D_2O exchange reflects a dramatic slowing in the overall rate so that the 800 cm^{-1} species reflects an earlier intermediate in the reaction sequence[96,98] (see below). Although this interpretation is counter to the more modest deuterium kinetic isotope effects observed by optical methods,[87] such an interpretation of the 785/800 cm^{-1} shift is intriguing and will require additional experimental study.

Both the 356 cm^{-1} and the 804 cm^{-1} species have controversial aspects in the reaction of the fully reduced enzyme with O_2. There is consensus that the 356 cm^{-1} intermediate appears early in the reaction sequence. Varotsis *et al.* have suggested that it arises from an intermediate that precedes oxygen−oxygen bond cleavage and assigned it to a ferric/cuprous/peroxy species;[74] a ferrous/cupric/peroxy formulation would also fit the data and may rationalize the anomolously low (Fe−O) stretching frequency in this species.[93] Kitagawa and co-workers favor a different view in which substrate bond cleavage occurs very early in the reaction.[96,98,104] In their interpretation, the 356 cm^{-1} mode is assigned to an Fe^{V}=O bending motion, which is unusual in both resonance enhancement properties and iron valence. Their assignment, however, is nicely supported by their recent observation that the oxygen in the oscillator can be exchanged with oxygen in solvent water.[98] This finding is difficult to rationalize within the context of a peroxy assignment for the 356 cm^{-1} mode (but see below). Thus, the structure of the 356 cm^{-1} intermediate continues to be debated. An unambiguous structure assignment would put a key piece of the oxidase puzzle into place.

The 804 cm^{-1} species is also problematic, but for different reasons. This species can be assigned, unambiguously, to a ferryl species on the basis of $^{16}O-^{18}O$ mixed-isotope experiments.[104] In the work from Kitagawa's lab on the fully reduced enzyme/O_2

Table 2. Assignment of Reaction Intermediates Found in the Reaction of Cytochrome *c* Oxidase with Dioxygen or Hydrogen Peroxide

mode ^{16}O, cm^{-1}	$\Delta^{16}O/^{18}O$ (cm^{-1})	$^{16}O-^{18}O$ sensitivity	$\Delta H^+/D^+$ (cm^{-1})	reaction[a]	assignment	comment	ref
358	−16			FR	$\nu_{Fe^{+3}-O}$	Fe^{+3}-O-O(H) species, precedes 785 cm^{-1} ferryl species	74
356	−14	none	0	FR, MV	$\delta_{His-Fe=O}$	individual Fe=O species, but closely follows the 804 cm^{-1} species (peroxy level)	94, 95, 96
355	−15			H_2O_2	$\delta_{His-Fe=O}$	individual Fe=O species, but closely follows the 785 cm^{-1} species (ferryl level), can be exchanged with bulk H_2O	97, 98
458	−24		−9	FR	$\nu_{Fe^{3+}-OH}$	final intermediate	74
450	−25		−7	FR	$\nu_{Fe^{3+}-OH}$	final intermediate	94, 95, 96
450	−25		−8	FR	$\nu_{Fe^{3+}-OH}$	final intermediate, single turnover	99
477	−18		−9	laser induced	$\nu_{Fe^{3+}-OH}$	multiple turnovers, pH <9, exchangeable with bulk H_2O	100
571	−25			FR, MV	$\nu_{Fe^{2+}-O_2}$	primary intermediate, develops more slowly for MV−CcO	71, 76
571	−27	567, 588	0	FR, MV	$\nu_{Fe^{2+}-O_2}$	primary intermediate, end-on complex	73, 94, 95, 96, 101
568	−21		0	FR, MV	$\nu_{Fe^{2+}-O_2}$	primary intermediate	72, 99, 102, 103
790	−35	none	10	FR	$\nu_{Fe^{4+}=O}$	H-bonded in H_2O	74, 78
785	−35	none	0	FR	$\nu_{Fe^{4+}=O}$	develops slowly in D_2O, not seen with MV−CcO	94, 95, 96, 101
786	−35	none	15	FR	$\nu_{Fe^{4+}=O}$	H-bonded in H_2O, deprotonated in D_2O	99
785	−35			H_2O_2	$\nu_{Fe^{4+}=O}$	"580 nm" form, closely accompanied by 355 cm^{-1} species, pK_a < 7 or > 10, can be exchanged with bulk H_2O, may contain several subspecies, develops slowly in D_2O	97, 98
804	−40	none	0	FR, MV	$\nu_{Fe^{5+}=O}$	peroxy level, closely accompanied by 356 cm^{-1} species	95, 96
804	−35	none	1.3	H_2O_2	$\nu_{Fe^{4+}=O}$	the "607 nm" form, neutral porphyrin, hydrogen bonded (pK_a > 10), non-exchangeable with bulk H_2O	97, 98

[a] FR, fully reduced; MV, mixed valence; H_2O_2, oxidized + H_2O_2 reaction.

reaction, this species appears early,[96] and in agreement with their work on the reaction of the oxidized enzyme with H_2O_2,[104] the Okazaki group assigns the 804 cm^{-1} species to an intermediate that is formally at the level of peroxide. They suggest that it arises from the stretching motion of an Fe^{V}=O species that is the immediate product of O=O bond cleavage; in essence, they propose that the 607 nm peroxy species, to which they assign an 804 cm^{-1} mode,[104] occurs as a well-populated intermediate in the reaction of the fully reduced enzyme with O_2. The postulated assignments and sequence of appearance for the discrete oxygen-isotope-sensitive modes observed by the Okazaki group are summarized in Figure 10a.

In contrast to the observations of the Okazaki group on the 804 cm^{-1} species, neither the Bell nor the East Lansing groups observe[122] the 804 cm^{-1} species clearly in the reaction of the reduced enzyme with O_2, although in some time-resolved spectra from both labs there do appear to be broadenings to the high-frequency side of the 785 cm^{-1} mode.[74,99] In addition, the East Lansing group has confirmed the Okazaki observation that the 804 cm^{-1} mode can be detected in the reaction of the mixed-valence enzyme with O_2 following decay of the initial oxy intermediate[96] (Pressler, M.; Floris, R.; Babcock, G. T., unpublished results). Taken together, these observations suggest that the 804 cm^{-1} peroxy species is not populated to a great extent in time-resolved experiments on the fully reduced enzyme/O_2 reaction carried out by either Rousseau and co-workers or by Varotsis *et al.* This is consistent with the optical work described above,[79,80,87,91] which confirms that oxy decay in the fully reduced enzyme reaction is largely through the oxidation of a^{2+}, which would minimize the population of the 804 cm^{-1} oscillator that lies along the 5000 s^{-1} branch in Figure 9. The current view of the intermediates that are detected by Raman in East Lansing is summarized in Figure 10b. Clearly, the assignment of the 356 cm^{-1} species to an iron−peroxide coupling conflicts with the Okazaki exchange data noted above; in light of the Proshlyakov *et al.* data,[104] this requires that oxygen−oxygen bond cleavage chemistry is reversible. Alternatively, the 356 cm^{-1} mode may arise from an oxygen-ligated Cu_B species, although the Okazaki group has argued against such an assignment.[96]

To conclude this section on the reaction of reduced cytochrome oxidase with dioxygen, considerable progress has been made in understanding the early steps in this process (Figure 9). Nonetheless, a good deal of uncertainty and controversy surrounds the nature of the intermediates and pathways that occur following the onset of proton control with the uptake of the 10^4 s^{-1} proton. An alternative approach to these issues has developed in parallel with time-resolved work on the fully reduced enzyme/O_2 reaction and is reviewed in the following section.

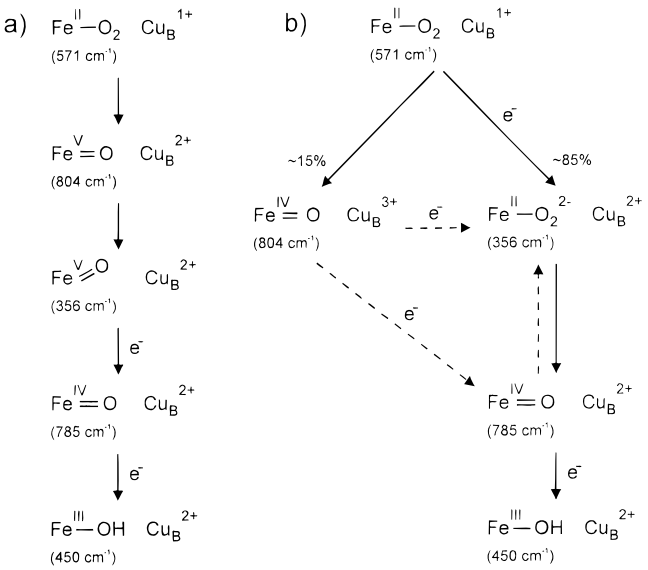

Figure 10. Alternative structural proposals for the oxygen isotope sensitive vibrations that are observed during the reaction of cytochrome oxidase with dioxygen in time-resolved resonance Raman measurements. Reaction sequences and the observed vibrational frequency and postulated structure for each of the intermediates are shown. Part a summarizes a recent model presented by Kitagawa and co-workers (see ref 96 and the text for details). Part b presents suggested structures in a reaction sequence proposed by Babcock and co-workers (see ref 48 and the text for details).

4. The Peroxy and Ferryl Levels in the Mixed-Valence Enzyme/O_2 and Oxidized-Enzyme/H_2O_2 Reactions

Considerable attention recently has focused on two intermediates that are formed in partial reactions of the terminal oxidase/O_2 mechanism. These are designated as Peroxy$_{607}$ and Ferryl in the simplified reaction scheme in Figure 7. The first of these two is characterized by a difference absorbance maximum, relative to the oxidized enzyme, at 607 nm in the visible region and is formed as the product of the O_2 reaction with the mixed-valence enzyme. Chance and co-workers, in their low-temperature trapping experiments, had observed a species with a similar red-shifted visible absorption maximum and had designated this species as compound **C**.[66] Wikström used highly oxidizing conditions and an electrochemical proton gradient induced by ATP addition to reverse electron flow through oxidase in mitochondrial preparations.[84] With this approach, he was able to drive one or two electrons from water or hydroxide through the enzyme to cytochrome *c*. The product of the one-electron reversal had an absorbance maximum at approximately 580 nm [difference extinction (580−630 nm) ≅ 5.3 mM^{-1} cm^{-1}]; the result of two-electron reversal yielded a 607 nm absorber [difference extinction (607−630 nm) ≅ 11 mM^{-1} cm^{-1}].[105] The postulated identification of the 607 nm absorber as compound **C** followed and a ferric peroxy structure was proposed. This species is commonly designated as "P" in the literature and as Peroxy$_{607}$ in Figure 7. The one-electron reversal species, with a difference absorbance maximum at ~580 nm, was postulated to have a Fe^{IV}=O structure and accordingly designated as "ferryl" or "F." This species is formally and, as formulated, structurally analogous to compounds **II** that occur in peroxidase catalysis.[84]

Intermediates with spectral properties resembling those of P and F could also be formed by addition of H_2O_2 to the resting enzyme. At mildly alkaline pH with low concentrations of peroxide, the predominant species is P; at higher peroxide concentrations, P is formed initially but is converted to the 580 nm absorbing F with time.[81−83] The optical properties of F are variable and the visible absorption maximum may shift over several nanometers as a function of pH. Nonetheless, the situation, until recently, looked reasonably clear: P and F species could be formed in a number of oxidase partial reactions, one-electron reduction of each was linked to proton translocation, and the structural assignments of P as a ferric peroxy intermediate and of F as a ferryl-oxo species seemed reasonably secure.[3] Although we have argued above that the P branch in the reaction of the fully reduced enzyme with O_2 is a relatively minor route at room temperature, this does not preclude the occurrence of a structure analogous to P as a precursor to the peroxy species **6** in the majority pathway in Figure 9.

Recent developments, however, have led to controversy regarding these valence and structural assignments for the P and F species. In the *bo*$_3$ terminal oxidases, for example, Watmough *et al*. had observed only a single intermediate in the reaction of peroxide with the enzyme. They suggested that this species was analogous to P and, from MCD spectra, assigned it an oxo ferryl structure.[106] Weng and Baker assigned both P and F to oxo ferryls but with an additional oxidizing equivalent stored as a radical in P.[107] Proshlyakov *et al*. have provided strong evidence in support of the occurrence of an oxo ferryl at the P level in their Raman studies of the oxidized enzyme/peroxy reaction.[104] With 607 nm excitation, they showed that an 804 cm^{-1} mode, which they could assign unequivocally to a ferryl species from $^{16}O-^{18}O$ mixed-isotope experiments, accompanied P formation. Subsequent work from the same group with Soret excitation also showed the occurrence of a 355 cm^{-1} oxygen isotope-sensitive mode and a 785 cm^{-1} ferryl species that followed F kinetics.[97,98] These are important experiments for at least two reasons. First, they establish that intermediates that occur during the reaction of the reduced enzyme with O_2 also appear to occur during the oxidized enzyme/H_2O_2 process, which establishes critical links between the two different reactions. Second, their data suggest that both P and F have ferryl-type structures and that, if P is one electron more oxidized than F, the additional oxidizing equivalent must be stored at a site other than heme a_3. Finally, Fabian and Palmer have studied the stoichiometry of P and F formation and have obtained data that suggest that both are two electrons more oxidizing than the resting enzyme. They suggested that P could be formulated as an $Fe_{a_3}^{IV}$=O/Cu_B^{3+} species and that F is a low-spin ferric heme a_3 peroxy adduct.[83] These recent experiments clearly have important implications for terminal oxidase chemistry. In particular, they

Table 3. Observed pK_a's for Selected Proton-Coupled Processes in Cytochrome Oxidase

process	pK_a	comments	ref.
reduction of binuclear center	(ox.) <7.2 (red.) >8.5	two H^+ taken up	88
reduction of a_3	(ox) <7.0 (red.) >9.0	H^+ uptake controls electron delivery to binuclear center	112
oxygen reduction, fully reduced enzyme, late kinetic phases	7.9	base postulated to occur in binuclear center	86, 87
H^+ uptake, O_2 reduction	8−8.5	base postulated to mediate H^+ transfer from medium to binuclear center	87
$a_3^{2+} \rightarrow a^{3+}$	(a_3^{3+}) = 8.5	base postulated to occur in binuclear center	25, 113, 114
back electron transfer following CO photodissociation	(a_3^{2+}) [(a_3^{3+}) 9.1 (a_3^{2+}) 10.3 *spheroides*]		
$A_3^{2+} \rightarrow a^{3+}$	~7.7	proton channel leading to binuclear center, average value	113, 114
back electron transfer following CO photolysis	[~8.7 *spharoides*]		

generate substantive questions regarding oxygen−oxygen bond cleavage chemistry, the occurrence of redox sites beyond Cu_A, Cu_B, and the two heme A chromophores, and the nature of the reactive species that drive proton pumping.

Many of the issues raised in these experiments remain to be resolved, although some clarification is beginning to emerge. Thus, Wikström and co-workers have demonstrated recently that, in the bo_3 quinol oxidases, two distinct intermediates with optical properties analogous to P and F can be generated.[108] In addition, Hirota *et al*. have shown that several of the oxygen isotope modes detected in the reaction of the mitochondrial aa_3 enzyme with O_2 can also be observed in the dioxygen reaction of the bo_3 quinol oxidase from *E. coli*.[118] Although most of the work on dioxygen reaction chemistry done so far has been carried out with the mitochondrial enzyme, these observations are reassuring in dispelling concerns that the quinol oxidase differed fundamentally, in terms of mechanism, from the cytochrome oxidases.[108,109] The Raman work that has been done on the oxidase partial reactions can be criticized (as can Raman on oxidase in general[91]), as the technique does not lend itself easily to quantitation, that is, a strong scatter in a minority species can easily dominate a spectrum. In the oxidase/H_2O_2 reactions, this criticism is made more poignant by the fact that it is difficult to prepare the P and F intermediates in pure form. Proshlyakov *et al*., however, are clearly aware of these difficulties and have buttressed their assignments by following optical and Raman spectra simultaneously and by tracking relative intensities of oxygen isotope sensitive modes in their Raman spectra with visible absorption features that they observed simultaneously.[97,98]

A more fundamental issue with the way in which the P and F intermediates are treated is the implicit assumption that each is a single homogeneous species. We have already noted above that the optical properties of these species are pH dependent, which indicates that a number of different species that are presumably connected by protonic equilibria contribute to P and F populations. Hill and Greenwood, in an early and insightful time-resolved optical study of the reaction of the mixed-valence enzyme with dioxygen, which is a common route to the production of P, noted the occurrence of at least two intermediates following the decay of the oxy species prior to the formation of the 607 nm absorber.[68] This early work and the current controversies that surround the assignment of the structures to the P and F forms of the enzyme suggest that a detailed study of the mixed-valence enzyme/O_2 system, as it evolves in time toward the 607 nm absorber, would be useful.

E. Proton Control, Proton-Coupled Electron Transfer, and Proton Pumps

Detailed proton-pumping models for the terminal oxidases have been proposed by Wikström and co-workers[40] and by Iwata *et al*.[10] that rely on a carefully orchestrated sequence of coupled proton and electron transfers (section B and Figure 2). In essence, proton transfers control the electron transfers, as we have stressed above, with the electroneutrality principle advanced by Rich and his co-workers providing the underlying driving force for the control.[41,88,110,111] At present, experimental information on these proton-coupled redox processes, on the amino acid side chains involved, and on the relevant pK_a's is sketchy, but experiments that address these issues are beginning to emerge. Directed mutagenesis is an incisive tool in this effort, particularly with the availability of the crystal structure of the enzyme, as described above (section B).

Direct stoichiometric, thermodynamic, and kinetic measurements are additional avenues into these questions, and several relevant experiments have been described recently. Several of these are summarized in Table 3. Mitchell and Rich have shown that reduction of the binuclear center is coupled to the uptake of two protons.[88] The pK_a's of these groups were not accessible over the pH range studied, indicating that their pK_a's are below 7 in the oxidized enzyme and greater than 8.5 in the reduced enzyme. Verkovsky *et al*. have noted similar behavior in their study of electron delivery to the binuclear center.[112] In their work, they showed that electron transfer from heme a^{2+} to heme a_3^{3+} is coupled to the protonation of a group with a redox-linked pK_a. In the oxidized enzyme, the pK_a of this species is less than 7 and, upon reduction, it shifts to a value greater than 9. The stoichiometric work of Mitchell and Rich and the kinetic/thermodynamic measurements of Verkhovsky *et al*. dovetail nicely and indicate that substantial redox Bohr effects are observed upon reduction of the oxidized enzyme.

For the reduced enzyme, the work of the Göteborg group reveals somewhat different behavior. The discussion above (section D.3) showed that the late phases in the reduction of dioxygen are proton-controlled and that the pK_a's of the groups involved, both those postulated to occur directly in the binuclear center and those proposed to mediate H^+ transfer to the dioxygen reduction site from solution, have pK_a's in the range of 8−8.5.[87] In a recent set of CO photolysis experiments, redox Bohr effects were observed for a group postulated to occur in the binuclear center that determines the extent of $a_3^{2+} \rightarrow a^{3+}$ back electron transfer.[113,114] With the a_3 center oxidized, a pK_a near 9 was observed; upon reduction, this value shifted up by roughly one pK_a unit. The pK_a value in the reduced state is consistent with the work in Table 3 on the reduction of the binuclear center. The elevated pK_a observed in the a_3^{3+} state in the CO photolysis work, however, suggests that the redox state of Cu_B, which is reduced in the reverse-electron-flow experiments but oxidized in the Mitchell and Rich and Verkhovsky *et al.* measurements, has a substantial influence on the extent of the redox Bohr effects. This conclusion could be interpreted to support the idea of a Cu_B-based proton pump.[10,40]

Brzezinski has recently presented an additional example of proton-controlled electron transfer in cytochrome oxidase in an insightful, quantitative analysis of electron transfer between Cu_A and the *a* and a_3 sites.[22,25] Although the distance separating the binuclear Cu_A site from the two hemes is quite similar (section B, Figure 1), the electron-transfer rate to heme *a* is substantially faster than that to heme a_3. Brzezinski attributes this selectivity in electron-transfer rate to a much larger reorganization energy (λ) associated with the reduction of a_3 than of *a*. The hydrophilicity that is necessary for the protonic equilibria at the a_3 center contributes significantly to the increased a_3 λ value, which slows electron transfer to this site and directs it, instead, to the low-spin heme *a* center.

The experiments described in this section and summarized in Table 3 represent the initial efforts to understand the complex interplay between proton and electron transfers that is necessary to construct and control an efficient redox-driven proton pump. Undoubtedly, work in this area will increase in the near future.

F. Conclusions

In activating and reducing dioxygen to water and in coupling the free energy released to proton translocations, cytochrome oxidase carries out two remarkable biochemical functions. The crystal structure is now available, and rapid progress has been made in bringing the enzyme under molecular biological control. These developments, coupled with the sophisticated biochemical and biophysical probes of function that we now have at hand, provide optimism that we will soon have a detailed understanding of the molecular mechanisms by which the enzyme operates. This knowledge will in turn be the basis for unravelling the complex regulatory processes that affect oxidase activity and efficiency in eukaryotic cells.

Acknowledgments

We thank Michelle Pressler, Denis Proshlyakov, Yuejun Zhen, Denise Mills, and Thomas Nilsson for help in preparing tables and figures for this review. The work on cytochrome oxidase that has been carried out in the authors' laboratories is supported by NIH GM26916 (S.F.M.) and NIH GM25480 (G.T.B.).

References

(1) Minireview Series, Cytochrome Oxidase; Ferguson-Miller, S., Ed. *J. Bioenerg. Biomembr.* **1993**, *25*, 69−188.
(2) Wikström, M.; Krab, K.; Saraste, M. *Cytochrome Oxidase—A Synthesis*; Academic Press: New York, 1981.
(3) Babcock, G. T.; Wikström, M. *Nature* **1992**, *356*, 301−309.
(4) Malmström, B. G. *Acc. Chem. Res.* **1993**, *26*, 332−338.
(5) Einarsdottir, O. *Biochim. Biophys. Acta* **1995**, *1229*, 129−147.
(6) Kitagawa, T.; Ogura, T. *Prog. Inorg. Chem.*, in press.
(7) Weindruch, R. *Sci. Am.* **1996**, *January*, 46−52.
(8) Wikström, M. *Nature* **1977**, *266*, 271−273.
(9) Keilin, D. *Proc. R. Soc. London, Ser. B* **1925**, *98*, 312.
(10) Iwata, S.; Ostermeier, C.; Ludwig, B.; Michel, H. *Nature* **1995**, *376*, 660−669.
(11) Tsukihara, T.; Aoyama, H.; Yamashita, E.; Tomizaki, T.; Yamaguchi, H.; Shinzawa-Itoh, K.; Nakashima, R.; Yaono, R.; Yoshikawa, S. *Science* **1995**, *269*, 1069−1074.
(12) Tsukihara, T.; Aoyama, H.; Yamashita, E.; Tomizaki, T.; Yamaguchi, H.; Shinzawa-Itoh, K.; Nakashima, R.; Yaono, R.; Yoshikawa, S. *Science* **1996**, *272*, 1136−1144.
(13) Wilmanns, M.; Lappalainen, P.; Kelly, M.; Sauer-Eriksson, E.; Saraste, M. *Proc. Natl. Acad. Sci. U.S.A.* **1995**, *92*, 11955−11959.
(14) Calhoun, M. W.; Thomas, J. W.; Hill, J. J.; Hosler, J. P.; Shapleigh, J. P.; Tecklenburg, M. M. J.; Ferguson-Miller, S.; Babcock, G. T.; Alben, J. O.; Gennis, R. B. *Biochemistry* **1993**, *32*, 10905−10911.
(15) Hosler, J. P.; Ferguson-Miller, S.; Calhoun, M. W.; Thomas, J. W.; Hill, J.; Lemieux, L.; Ma, J.; Georgiou, C.; Fetter, J.; Shapleigh, J. P.; Tecklenburg, M. M. J.; Babcock, G. T.; Gennis, R. B. *J. Bioenerg. Biomembr.* **1993**, *25*, 121−136.
(16) Thomas, J. W.; Puustinen, A.; Alben, J. O.; Gennis, R. B.; Wikström, M. *Biochemistry* **1993**, *32*, 10923−10928.
(17) Fetter, J. R.; Qian, J.; Shapleigh, J.; Thomas, J. W.; García-Horsman, J. A.; Schmidt, E.; Hosler, J.; Babcock, G. T.; Gennis, R. B.; Ferguson-Miller, S. *Proc. Natl. Acad. Sci. U.S.A.* **1995**, *92*, 1604−1608.
(18) García-Horsman, J. A.; Puustinen, A.; Gennis, R. B.; Wikström, M. *Biochemistry* **1995**, *34*, 4428−4433.
(19) Woodruff, W. H. *J. Bioenerg. Biomembr.* **1993**, *25*, 177 −188.
(20) Rousseau, D. L.; Ching, Y.-C.; Wang, J. *J. Bioenerg. Biomembr.* **1993**, *25*, 165−176.
(21) Mitchell, D. M.; Ädelroth, P.; Hosler, J. P.; Fetter, J. R.; Brzezinski, P.; Pressler, M. A.; Aasa, R.; Malmström, B. G.; Alben, J. O.; Babcock, G. T.; Gennis, R. B.; Ferguson-Miller, S. *Biochemistry* **1996**, *35*, 824−828.
(22) Ramirez, B. E.; Malmström, B. G.; Winkler, J. R.; Gray, H. B. *Proc. Natl. Acad. Sci. U.S.A.* **1995**, *92*, 11949−11951.
(23) Hill, B. C. *J. Biol. Chem.* **1991**, *266*, 2219−2226.
(24) Pan, L. P.; Hibdon, S.; Liu, R.-Q.; Durham, B.; Millett, F. *Biochemistry* **1993**, *32*, 8492−8498.
(25) Brzezinski, P. *Biochemistry* **1996**, *35*, 5611−5615.
(26) Moser, C. C.; Keske, J. M.; Warncke, K.; Farid, R. S.; Dutton, P. L. *Nature* **1992**, *355*, 796−802.
(27) Zickermann, V.; Verkhovsky, M.; Morgan, J.; Wikstrom, M.; Anemuller, S.; Bill, E.; Steffens, G.; Ludwig, B. *Eur. J. Biochem* **1995**, *234*, 686−693.
(28) Zhen, Y. J.; Fetter, J.; Ferguson-Miller, S. *Biophys. J.* **1996**, *70*, A353.
(29) Gelles, J.; Blair, D. F.; Chan, S. I. *Biochim. Biophys. Acta* **1987**, *853*, 205−236.
(30) Hosler, J. P.; Shapleigh, J. P.; Tecklenburg, M. M. J.; Thomas, J. W.; Kim, Y.; Espe, M.; Fetter, J.; Babcock, G. T.; Alben, J. O.; Gennis, R. B.; Ferguson-Miller, S. *Biochemistry* **1994**, *33*, 1194−1201.
(31) Hosler, J. P.; Espe, M. P.; Zhen, Y.; Babcock, G. T.; Ferguson-Miller, S. *Biochemistry* **1995**, *34*, 7586−7592.
(32) Verkhovskaya, M.; Verkhovsky, M.; Wikström, M. *J. Biol. Chem.* **1992**, *267*, 14559−14562.

(33) Fetter, J. R.; Sharpe, M.; Qian, J.; Mills, D.; Ferguson-Miller, S.; Nicholls, P. *FEBS Lett.*, in press.
(34) Geren, L. M.; Beasley, J. R.; Fine, B. R.; Saunders, A. J.; Hibdon, S.; Pielak, G. J.; Durham, B.; Millett, F. *J. Biol. Chem.* **1995**, *270*, 2466−2662.
(35) Roberts, V. A.; Freeman, H. C.; Olson, A. J.; Tainer, J. A.; Getzoff, E. D. *J. Biol. Chem.* **1991**, *266*, 13431−13441.
(36) Ferguson-Miller, S.; Brautigan, D. L.; Margoliash, E. *J. Biol. Chem.* **1978**, *253*, 149−159.
(37) Pelletier, H.; Kraut, J. *Science* **1992**, *258*, 1748−1755.
(38) Miller, M. A.; Geren, L.; Han, G. W.; Saunders, A.; Beasley, J.; Pielak, G. J.; Durham, B.; Millett, F.; Kraut, J. *Biochemistry* **1996**, *35*, 667 −673.
(39) Wang, Y.; Margoliash, E. *Biochemistry* **1995**, *34*, 1948−1958.
(40) Wikström, M.; Bogachev, A.; Finel, M.; Morgan, J. E.; Puustinen, A.; Raitio, M.; Verkhovskaya, M. L.; Verkhovsky, M. I. *Biochim. Biophys. Acta* **1994**, *1187*, 106−111.
(41) Rich, P. R. *Aust. J. Plant Physiol.* **1995**, *22*, 479−484.
(42) Thomas, J. W.; Lemieux, L. J.; Alben, J. O.; Gennis, R. B. *Biochemistry* **1993**, *32*, 11173−11180.
(43) Hosler, J. P.; Shapleigh, J. P.; Mitchell, D. M.; Kim, Y.; Pressler, M. A.; Georgiou, C.; Babcock, G. T.; Alben, J. O.; Ferguson-Miller, S.; Gennis, R. B. *Biochemistry*, in press.
(44) Kadenbach, B.; Shroh, A.; Hüther, F.-J.; Reimann, A.; Steverding, D. *J. Bioenerg. Biomembr.* **1991**, *23*, 321−334.
(45) Frank, V.; Kadenbach, B. *FEBS Lett.* **1996**, *382*, 121 −124.
(46) Suarez, M. D.; Revzin, A.; Narlock, R.; Kempner, E. S.; Thompson, D. A.; Ferguson-Miller, S. *J. Biol. Chem.* **1984**, *259*, 13791−13799.
(47) Watanabe, Y.; Groves, J. T. *The Enzymes*; Sigman, S., Ed.; Academic: San Diego, 1992; pp 405−452.
(48) Babcock, G. T.; Floris, R.; Nilsson, T.; Pressler, M.; Varotsis, C.; Vollenbroek, E. *Inorg. Chim. Acta* **1996**, *243*, 345−353.
(49) Lee, S.-K.; Fox, B. G.; Froland, W. A.; Lipscomb, J. D.; Münck, E. *J. Am. Chem. Soc.* **1993**, *115*, 6450−6451.
(50) Liu, K. E.; Valentine, A. M.; Wang. D.; Huynh, B. H.; Edmondson, D. E.; Salioglu, A.; Lippard, S. J. *J. Am. Chem. Soc.* **1995**, *117*, 10174−10185.
(51) Edmondson, D. E.; Huynh, B. H. *Inorg. Chim. Acta*, in press.
(52) Liu, Y.; Nesheim, J. C.; Lee, S.-K.; Lipscomb, J. D. *J. Biol. Chem.* **1995**, *270*, 24662−24665.
(53) Babcock, G. T. In *Proceedings of Stable Isotope Applications in Biomolecular Structure and Mechanisms*; Trewhilla, J., Cross, T. A., Unkefer, C. J., Eds.; Los Alamos National Laboratory Reports, LA-12893-C, 1994; pp 15−26.
(54) Wikström, M. *Nature* **1989**, *338*, 776−778.
(55) Babcock, G. T.; Varotsis, C. *Proc. SPIE−Int. Soc. Opt. Eng. Biomol. Spectrosc.* (III), **1993**, *1890*, 104−113.
(56) Rétey, J. *Angew. Chem., Int. Ed. Engl.* **1990**, *29*, 355−361.
(57) Gibson, Q.; Greenwood, C. *Biochem. J.* **1963**, *86*, 541−554.
(58) Greenwood, C.; Gibson, Q. H. *J. Biol. Chem.* **1967**, *242*, 1782−1787.
(59) Alben, J. O.; Moh, P. P.; Fiamingo, F. G.; Altschuld, R. A. *Proc. Natl. Acad. Sci. U.S.A.* **1981**, *78*, 234−237.
(60) Fiamingo, F. G.; Altschuld, R. A.; Moh, P. P.; Alben, J. O. *J. Biol. Chem.* **1982**, *257*, 1639−1650.
(61) Blackmore, R. S.; Greenwood, C.; Gibson, Q. H. *J. Biol. Chem.* **1991**, *266*, 19245−19249.
(62) Dyer, R. B.; Einarsdóttir, Ó.; Killough, P. M.; López-Garriga, J. J.; Woodruff, W. H. *J. Am. Chem. Soc.* **1989**, *111*, 7657−7659.
(63) Woodruff, W. H.; Einarsdóttir, Ó.; Dyer, R. B.; Bagley, K. A.; Palmer, G.; Atherton, S. J.; Goldbeck, R. A.; Dawes, T. D.; Kliger, D. S. *Proc. Natl. Acad. Sci. U.S.A.* **1991**, *88*, 2588−2592.
(64) Einarsdóttir, Ó.; Dyer, R. B.; Lemon, D. D.; Killough, P. M.; Hubig, S. M.; Atherton, S. J.; López-Garriga, J. J.; Palmer, G.; Woodruff, W. H. *Biochemistry* **1993**, *32*, 12013−12024.
(65) Lemon, D. D.; Calhoun, M. W.; Gennis, R. B.; Woodruff, W. H. *Biochemistry* **1993**, *32*, 11953−11956.
(66) Chance, B.; Saronio, C.; Leigh, J. S., Jr. *J. Biol. Chem.* **1975**, *150*, 9226−9237.
(67) Clore, M. G.; Andréasson, L.-E.; Karlsson, B. G.; Aasa, R.; Malmström, B. *Biochem. J.* **1980**, *185*, 139−154.
(68) Hill, B. C.; Greenwood, C. *Biochem. J.* **1984**, *218*, 913−921.
(69) Hill, B. C.; Greenwood, C.; Nicholls, P. *Biochim. Biophys. Acta* **1986**, *853*, 91−113.
(70) Babcock, G. T.; Jean, J. M.; Johnston, L. N.; Palmer, G.; Woodruff, W. H. *J. Am. Chem. Soc.* **1984**, *106*, 8305−8306.
(71) Varotsis, C.; Woodruff, W. H.; Babcock, G. T. *J. Am. Chem. Soc.* **1989**, *111*, 6439−6440; *112*, 1297.
(72) Han, S.; Ching, Y.-C.; Rousseau, D. L. *Proc. Natl. Acad. Sci. U.S.A.* **1990**, *87*, 2491−2495.
(73) Ogura, T.; Takahashi, S.; Shinzawa-Itoh, K.; Yoshikawa, S.; Kitagawa, T. *J. Am. Chem. Soc.* **1990**, *112*, 5630−5631.
(74) Varotsis, C.; Zhang, Y.; Appelman, E. H.; Babcock, G. T. *Proc. Natl. Acad. Sci. U.S.A.* **1993**, *90*, 237−241.
(75) Oertling, W. A.; Kean, R. T.; Wever, R.; Babcock, G. T. *Inorg. Chem.* **1990**, *29*, 2633−2645.
(76) Varotsis, C.; Woodruff, W. H.; Babcock, G. T. *J. Biol. Chem.* **1990**, *265*, 11131−11136.
(77) Han, S.; Ching, Y.-C.; Rousseau, D. L. *Proc. Natl. Acad. Sci. U.S.A.* **1990**, *87*, 8408−8412.
(78) Varotsis, C.; Babcock, G. T. *Biochemistry* **1990**, *29*, 7357−7362.
(79) Oliveberg, M.; Brzezinski, P.; Malmström, B. G. *Biochim. Biophys. Acta* **1989**, *977*, 322−328.
(80) Verkhovsky, M. I.; Morgan, J. E.; Wikström, M. *Biochemistry* **1994**, *33*, 3079−3086.
(81) Bickar, D.; Bonaventura, J.; Bonaventura, C. *Biochemistry* **1982**, *24*, 2661−2666.
(82) Konstantinov, A. A.; Capitanio, N.; Uygodina, T. V.; Papa, S. *FEBS Lett.* **1992**, *312*, 71−74.
(83) Fabian, M.; Palmer, G. *Biochemistry* **1995**, *34*, 13802−13810.
(84) Wikström, M. *Proc. Natl. Acad. Sci. U.S.A.* **1981**, *78*, 4051−4054.
(85) Wikström, M.; Morgan, J. E. *J. Biol. Chem.* **1992**, *267*, 10266−10273.
(86) Oliveberg, M.; Hallén, S.; Nilsson, T. *Biochemistry* **1991**, *30*, 436−440.
(87) Hallén, S.; Nilsson, T. *Biochemistry* **1992**, *31*, 11853−11859.
(88) Mitchell, R.; Rich, P. R. *Biochim. Biophys. Acta* **1994**, *1186*, 19−26.
(89) Rich, P. R.; Moody, A. J. In *Bioelectrochemistry: Principles and Practice*; Graber, P., Ed.; Elsevier: Amsterdam, in press.
(90) Varotsis, C. A.; Babcock, G. T. *J. Am. Chem. Soc.* **1995**, *117*, 11260−11269.
(91) Hill, B. C. *J. Biol. Chem.* **1994**, *269*, 2419−2425.
(92) Oliveberg, M.; Malmström, B. G. *Biochemistry* **1992**, *31*, 3560−3563.
(93) Blair, D. F.; Witt, S. N.; Chan, S. I. *J. Am. Chem. Soc.* **1985**, *107*, 7389−7399.
(94) Ogura, T.; Takahashi, S.; Shinzawa-Itoh, K.; Yoshikawa, S.; Kitagawa, T. *Bull. Chem. Soc. Jpn.* **1991**, *64*, 2901−2907.
(95) Ogura, T.; Takahashi, S.; Hirota, S.; Shinzawa-Itoh, K.; Yoshikawa, S.; Appelman, E. H.; Kitagawa, T. *J. Am. Chem. Soc.* **1993**, *115*, 8527−8536.
(96) Ogura, T.; Hirota, S.; Shinzawa-Itoh, K.; Yoshikawa, S.; Kitagawa, T. *J. Am. Chem. Soc.* **1996**, *118*, 5443−5449.
(97) Proshlyakov, D. A.; Ogura, T.; Shinzawa-Itoh, K.; Yoshikawa, S.; Kitagawa, T. *Biochemistry* **1996**, *35*, 76−82.
(98) Proshlyakov, D. A.; Ogura, T.; Shinzawa-Itoh, K.; Yoshikawa, S.; Kitagawa, T. *Biochemistry* **1996**, *35*, 8580−8586.
(99) Han, S.; Ching, Y.; Rousseau, D. L. *Nature* **1990**, *348*, 89−90.
(100) Han, S.; Ching, Y.; Rousseau, D. L. *J. Biol. Chem.* **1989**, *264*, 6604−6607.
(101) Ogura, T.; Takahashi, S.; Shinzawa-Itoh, K.; Yoshikawa, S.; Kitagawa, T. *J. Biol. Chem.* **1990**, *265*, 14721−14723.
(102) Han, S.; Ching, Y.; Rousseau, D. L. *J. Am. Chem. Soc.* **1990**, *112*, 9445−9451.
(103) Takahashi, S.; Ching, Y.; Wan, J.; Rousseau, D. L. *J. Biol. Chem.* **1995**, *270*, 8405−8407.
(104) Proshlyakov, D. A.; Ogura, T.; Shinzawa-Itoh, K.; Yoshikawa, S.; Appelman, E. H.; Kitagawa, T. *J. Biol. Chem.* **1994**, *269*, 29385−29388.
(105) Wikström, M.; Morgan, J. E. *J. Biol. Chem.* **1992**, *267*, 10266−10273.
(106) Watmough, N. J.; Cheesman, M. R.; Greenwood, C.; Thomson, A. J. *Biochem. J.* **1994**, *300*, 469−475.
(107) Weng, L.; Baker, G. M. *Biochemistry* **1991**, *30*, 5727−5733.
(108) Morgan, J. E.; Verkhovsky, M. I.; Puustinen, A.; Wikström, M. *Biochemistry* **1995**, *34*, 15633−15637.
(109) Puustinen, A.; Verkhovsky, M. I.; Morgan, J. E.; Belevich, N. P.; Wikström, M. *Proc. Natl. Acad. Sci. U.S.A.* **1996**, *93*, 1545−1548.
(110) Mitchell, R.; Mitchell, P.; Rich, P. R. *Biochim. Biophys. Acta* **1992**, *1101*, 188−191.
(111) Musser, S. M.; Chan, S. I. *Biophys. J.* **1995**, *68*, 2543−2555.
(112) Verkhovsky, M. I.; Morgan, J. E.; Wikström, M. *Biochemistry* **1995**, *34*, 7483−7491.
(113) Hallén, S.; Brzezinski, P.; Malmström, B. G. *Biochemistry* **1994**, *33*, 1467−1472.
(114) Ädelroth, P.; Brzezinski, P.; Malmström, B. G. *Biochemistry* **1995**, *34*, 2844−2849.
(115) Riistama, S.; Puustinen, A.; Garcia-Horseman, A.; Iwata, S.; Michel, H.; Wikström, M. *Biochim. Biophys. Acta* **1996**, *1275*, 1−4.
(116) Taanman, J.-W.; Turina, P.; Capaldi, R. *Biochemistry* **1994**, *33*, 11833−11841.
(117) Verkhovsky, M. I.; Morgan, J.; Puustinen, A.; Wikström, M. *Nature* **1996**, *380*, 268−270.
(118) Hirota, S.; Mogi, T.; Ogura, T.; Hirano, T.; Anraku, Y.; Kitagawa, T. *FEBS Lett.* **1994**, *352*, 67−70.
(119) Fann, Y.; Ahmed, I.; Blackburn, N.; Boswell, J.; Verkhovskaya, M.; Hoffman, B.; Wikström, M. *Biochemistry* **1995**, *34*, 10245−10255.
(120) Powers, L.; Chance, B.; Ching, Y.; Angiolillo, P. *Biophys. J.* **1981**, *34*, 465−498.
(121) Scott, R. A.; Li, P. M.; Chan, S. I. *Ann. N.Y. Acad. Sci.* **1988**, *550*, 53−58.
(122) It is useful to consider, briefly, some technical aspects of the way in which time-resolved Raman has been implemented by the groups involved. Both Kitagawa's group and Rousseau's use

continuous-wave (cw) sources and achieve time resolution by displacing the CO photodissociating beam and the probe beam spatially along a flow tube. This approach has the advantage of using cw lasers, which provide high-quality Raman spectra, but the disadvantage that the time resolution may be blurred by laminar flow effects. Babcock's group uses two ns-pulsed lasers to achieve time resolution, which has the advantage of avoiding laminar flow issues and providing very accurate time resolution, but the disadvantage of the poorer beam quality of pulsed lasers, which leads to lower signal/noise ratios. Both Rousseau's and Babcock's group use a single pass through their spectrometer, whereas Kitagawa's group uses a recycling system that allows multiple passes of the enzyme through their detection system. While conserving enzyme, the latter approach introduces the possibility that full reduction of the protein is not achieved on each pass through the apparatus.

CR950051S